

Published in final edited form as:

Blood. 2011 December 22; 118(26): e192–e208. doi:10.1182/blood-2011-04-345330.

Transcriptomic analyses of murine resolution-phase macrophages

Melanie J. Stables¹, Sonia Shah², Evelyn B. Camon³, Ruth C. Lovering³, Justine Newson¹, Jonas Bystrom⁴, Stuart Farrow⁵, and Derek W. Gilroy¹

¹Centre for Clinical Pharmacology and Therapeutics, Division of Medicine, 5 University Street, University College London, London WC1E 6JJ, United Kingdom

²UCL Genetics Institute, Room 212, Darwin Building, Gower Street, WC1E 6BT

³Centre for Cardiovascular Genetics, Dept Medicine, University College London, 5 University St, London WC1E 6JF, UK

⁴Translational Medicine & Therapeutics, William Harvey Research Institute, Barts & the London, Queen Mary, University of London, Charterhouse Square, London EC1M 6BQ

⁵Respiratory CEDD, GlaxoSmithKline, Stevenage SG1 2NY, UK

Abstract

Macrophages are either classically (M1) or alternatively-activated (M2). While this nomenclature was generated from monocyte-derived macrophages treated *in vitro* with defined cytokine stimuli, the phenotype of *in vivo*-derived macrophages is less understood. We completed Affymetrix-based transcriptomic analysis of macrophages from the resolution-phase of a zymosan-induced peritonitis. Compared to macrophages from hyper-inflamed mice possessing a pro-inflammatory nature as well as naive macrophages from the un-inflamed peritoneum, resolution-phase macrophages (rM) are similar to monocytes-derived dendritic cells (DC), being CD209a positive but lack CD11c. They are enriched for antigen processing/presentation (MHC-II [H2-Eb1, H2-Ab1, H2-Ob, H2-Aa], CD74, CD86), secrete T- and B-lymphocyte chemokines (Xcl1, Ccl5, Cxcl13) as well as factors that enhance macrophage/DC development and promote DC/T cells synapse formation (Clec2i, Tnfsf4, Clcf1). rM are also enriched for cell cycle/proliferation genes as well as Alox15, Timd4 and Tgfb2, key systems in the termination of leukocyte trafficking and clearance of inflammatory cells. Finally, comparison with *in vitro*-derived M1/M2 shows that rM are neither classically nor alternatively activated but possess aspects of both definitions consistent with an immune regulatory phenotype. We propose that macrophage *in situ* cannot be rigidly categorised as they can express many shades of the inflammatory spectrum determined by tissue, stimulus and phase-of-inflammation.

Introduction

Macrophages are defined as either pro- or anti-inflammatory thereby promoting or dampening innate/adaptive immunity¹. Specifically, macrophages may dispose of necrotic

Address correspondence to DWGilroy. d.gilroy@ucl.ac.uk; fax +020-7679-6351.

or apoptotic material², phagocytose and kill infectious organisms³, present peptide antigens to lymphocytes⁴ as well as degrade/synthesise components of the extracellular matrix thereby modulating tissue repair and wound healing⁵. In summary, macrophages possess diverse functions as well as a plastic phenotype commensurate with their inflammatory environment. Moreover, macrophages are central to the aetiology of many diseases driven by inflammation including atherosclerosis, rheumatoid arthritis, chronic obstructive pulmonary disease, asthma and carcinogenesis, for instance. Thus, altering pathogenic macrophages may subvert ongoing inflammatory responses down a resolution/tissue repair pathway.

Macrophages, depending on the micro-environment, may become classically activated (M1) acquiring a pro-inflammatory phenotype or alternatively activated with the latter further subdivided into M2a, M2b or M2c⁶. Regulatory macrophages (M2b), generated in response to immune complexes have been described⁷, which along with M2 cells are immune-suppressive. However, macrophage inflammatory characteristics has largely being garnered from monocytes differentiated *in vitro* in response to defined stimuli and the phenotype of macrophages in tissues in various phases of the inflammatory response (onset versus resolving; adaptive versus tissue injury) is little understood. Indeed, we suspect, as have others⁷ that macrophage plasticity gives rise to a broad range of subtly different phenotypes that may be stimulus, disease, tissue and phase-of-inflammation specific. Addressing this in the context of self-limiting inflammation we found previously that macrophages isolated from a resolving peritonitis elicited by yeast cell wall extract (zymosan), possess a hybrid M1/M2⁸. Therefore, we aimed to get a more definitive image of macrophages during resolving acute inflammatory responses using Affymetrix-based mRNA transcriptomic analysis. It transpires that macrophage involved in the resolution of acute peritonitis, compared to naive as well as macrophage isolated from septic mice and therefore assumed to have an pro-inflammatory phenotype, are specifically enriched for the biochemical machinery necessary for proliferation as well as antigen processing and presentation, secretion of T- and B-lymphocyte chemokines and factors that enhance macrophage/DC development and promote DC/T cells synapse formation. Not surprisingly, they also have elevated levels of genes involved in dampening leukocyte trafficking, efferocytosis and wound repair.

Material and Methods

Reagents

Recombinant mouse cytokines were from Invitrogen (IFN γ and M-CSF) or Peprotech (IL-4). LPS from *Salmonella typhosa* was from Sigma-Aldrich. FACS antibodies were from either BD biosciences (CD11b, CD11c, Ly6c, CD19, MHC-II, CD86 and CD62L) or eBiosciences (F4/80 and 7/4 Antigen). All chemicals used were from Sigma-Aldrich, unless specified.

Animal maintenance and induction of peritonitis

Male C57Bl6/J were bred in individual ventilated cages and maintained in a 12h/12h light/dark cycle at 22 \pm 1°C and given food and tap water *ad libitum* in accordance with UK Home Office regulations. Peritonitis was induced by the intraperitoneal injection of 0.1 or

10mg/mouse zymosan A. All mouse experiments were approved under a UK Home Office Project Licence.

Purification of peritoneal macrophages

Peritoneal cells were obtained by lavage with 3% sodium citrate before/at specific time-points after zymosan injection (see Results). Upon removal from the peritoneum, red blood cells were lysed using ACK lysing buffer (Lonza). B cells were removed using anti-CD19 microbeads (Miltenyi Biotech) according to manufacturer's instructions. Macrophages were further purified by adherence to culture plates in DMEM supplemented with 10% FBS, 2% L-glutamine and 1% penicillin/streptomycin (all Invitrogen) for 1h at 37°C in 5% CO₂. After which time, non-adherent cells (T-lymphocytes and neutrophils) were washed off (3X) using cold sterile PBS (Invitrogen) leaving greater than 98% macrophage purity. See also Figure S1 C and D.

Purification of splenic dendritic cells

Isolated murine spleen was injected with 0.5ml collagenase D (2mg/ml, Roche Diagnostics) and HEPES (10mM, Invitrogen), cut into smaller pieces and incubated using at 37°C for 30min. Subsequent material was passed through a 70µm cell strainer (BD Falcon) and collected cells were depleted of red blood cells using ACK lysing buffer. Splenic DCs were then purified using pan DC microbeads (Miltenyi Biotech) according to manufacturer's instructions. Three subpopulations of splenic dendritic cells (plasmacytoid, CD8α⁺ and CD8α⁻) were further purified using flow cytometric cell sorting (see 'FACS analysis and cell sorting' section below for details).

Generation and activation of bone marrow-derived macrophages (BMDM) and dendritic cells (BMDC)

BMDM and BMDC were obtained from femurs of 8-10 week-old C57Bl6/J. Cells were cultured in DMEM supplemented with 10% FBS, 1% penicillin/streptomycin, 20mM HEPES (all Invitrogen) and recombinant mouse M-CSF (10ng/ml) (BMDM) or GM-CSF (20ng/ml) and IL-4 (20ng/ml) for 7 days. Medium including M-CSF or GM-CSF and IL-4 was changed once on day 4. On day 7, live adherent cells were removed from plate using cell dissociation buffer, counted and re-suspended in complete DMEM. BMDM were then seeded onto standard 24-well plates and stimulated for 24h with both IFN-γ (20ng/ml) and LPS (100ng/ml, *Salmonella typhosa*) or IL-4 (20ng/ml) for M1 and M2 polarisation, respectively. In parallel, un-polarised macrophages were cultured in complete medium alone. BMDC were seeded onto standard 24-well plates and activated with LPS (100ng/ml) and 20nM MHC-II restricted ovalbumin (OVA) peptide (ISQVHAAHAEINEAGR; OVA₃₂₃₋₃₃₉) for 24h.

RNA preparation

Peritoneal macrophages and BMDM were subjected to RNA extraction using RNeasy micro or mini kit (Qiagen) as per manufacturer's protocol. Contaminating DNA was then removed by DNase I treatment (Qiagen).

Microarray analysis

RNA quality assessment and microarray analysis were performed at UCL's Wolfson Institute for Biomedical Research, Microarray Facility. Total RNA was quantified using Nanodrop 1000 Spectrophotometer and Agilent Bioanalyzer. RNA samples with RNA Integrity Number (RIN) > 8.5 were chosen to be prepped for further analysis. Total starting RNA material of 40ng was prepped using the NuGEN Ovation Pico WTA and fragmentation and labelling of the SPIA-cDNA was carried out using the NuGEN FL-Ovation Biotin V2. Fragmented and labelled SPIA-cDNA (5ug) was then hybridised to Affymetrix GeneChip Mouse Genome 430 2.0 Array (as per NuGEN instructions) for 16 hours at 45°C. Arrays were washed and stained using the GeneChip Fluidics Station 450 and scanned using the Affymetrix GeneChip Scanner. Data were normalised using the RMA normalisation algorithm in Expression Console 1.1 which was also used to assess quality metrics. Data was submitted to Gene Express, accession number E-MEXP-3189.

Pre-processing, gene expression analysis and bio-informatics

Sample pre-processing, gene expression analysis and functional enrichment analysis is described in detail in supplementary to material and methods.

Gene expression analysis by real-time PCR

Real-time PCR was performed after 500ng RNA was reverse transcribed (using Mouse Moloney Leukaemia Virus reverse transcriptase). 3ng cDNA was submitted to quantitative real-time PCR (Applied Biosystems 7900HT) with primer pairs listed in Table S1A-C and quantified using PowerSYBR® green (Applied Biosystems) following the manufacturer's instructions. Dissociation curve analysis was performed at 40 cycles to verify the identity of PCR product. For data analysis, the comparative threshold cycle (C_T) values for constitutively expressed cyclophilin (CYPH) were used to normalise loading variations and are expressed as arbitrary units (AU).

FACS analysis and cell sorting

400,000 total peritoneal cells re-suspended in FACS buffer (5% FBS in PBS) were incubated with antibodies (Table S2) for 30 min in the dark at 4°C. Cells were washed 3 times using wash buffer (1% FBS in PBS). In some instances, cells were then re-suspended in 1% FBS in PBS and incubated with streptavidin beads (V500 or PE, Becton Dickinson [BD]) for 20 min in the dark at 4°C. Again, cells were washed 3 times with 1% FBS in PBS and fixed with 0.1% paraformaldehyde. Control samples were generated using fluorescence minus one (FMO) controls. In cell sort experiments, monocytes and macrophages were sorted from a population of CD19⁻ cells as either Ly6c⁺F480⁺ and Ly6c⁻F480⁺. Three distinct populations of splenic DCs were sorted from CD19⁻ and CD3⁻ cells as either CD11c^{int}CD45R⁺, CD11c^{hi}CD205⁻ or CD11c^{hi}CD205⁺. Tests performed after both sorts have shown that these populations are >95% pure. All samples were analyzed on a FACS- LSRII or Fortessa or sorted in a FACS-Aria (both BD Biosciences). Flow cytometry analysis was completed using FlowJo (Tree Star Inc).

Statistical analysis of real-time PCR

Results are expressed as means \pm SEM. Differences between results were evaluated by one-way ANOVA and Bonferroni post-hoc analysis. Differences were considered significant when $P < 0.05$. Statistical analysis was performed using GraphPad Prism 5.

Results

Experimental model

We established two separate models of acute inflammation; one triggered by 0.1mg zymosan resulting in inflammation peaking in severity at 12h and resolving thereafter and another triggered by 10mg zymosan (Figure S2)8. Inflammation in the latter was maximal at 72h and associated with a systemic inflammatory response that persisted for up to three weeks as defined by elevated plasma cytokines. Arising from local anti-inflammatory/ immunosuppressive cues, we reasoned that macrophages from the resolution phase (48h onwards) of inflammation triggered by 0.1mg zymosan would possess a pro-resolution phenotype (rM) while those from the same time frame from 10mg zymosan would have an M1-like phenotype, hereafter referred to as pro-inflammatory macrophages. We also included macrophages from the naive peritoneum (un-inflamed) as well as macrophages from the intermediate time points of the resolving inflammation (0.1mg zymosan). Thus, resolving and non-resolving inflammation was induced in mice using two separate doses of zymosan (0.1mg & 10mg) and peritoneal macrophages collected at 5 time points (0hr, 4hr, 24hr, 48hr & 72hr). At each time point, gene expression was measured for 6 biological replicates using the Affymetrix mouse 430 2.0 arrays.

Differential Gene Expression Analysis

In the first instance we compared rM against pro-inflammatory macrophages (Figure 1A) using cells from 6 separate animals in each group with gene expression in each showing a clear dichotomy in macrophage phenotypes. Figure 1B reveals a sample of the top 20 most differentially expressed genes in rM cells versus pro-inflammatory macrophages based upon FDR of 0.001 and fold expression difference of 2. Up-regulated genes include 15-lipoxygenase (Alox15) and T-cell immunoglobulin and mucin domain containing 4 (Timd4), which are responsible for halting leukocyte trafficking^{9,10} and the recognition/phagocytosis of apoptotic cells¹¹; key determinant of resolution. Tgfb2 and latent Tgfb2 along with the T/B cell chemoattractant Cxcl13 are also highly expressed in rM compared to inflammatory macrophages as well as cyclin B2 (Ccnb2). We also report a down-regulation of genes associated with inducing inflammation such as cathepsin K (Ctsk), Il-1 family, member 9 (Il1f9), and metalloprotease 8 (Mmp9), Figure 1B.

We next used the CLICK algorithm on the software package Expander to identify significant functional enrichment in genes differentially expressed in rM versus pro-inflammatory macrophages. A 5% false discovery rate and fold change greater than 1.5 revealed 2661 probesets up-regulated in rM. This analysis found 175 genes involved in proliferation (Figure 1C) including cell cycle (GO: 0007049), cell division (GO: 0051301), cell cycle processes (GO: 0022402), M phase (GO: 0000279), nuclear division (GO: 0000280) and mitotic cell division (GO: 0000278). We entered these 175 genes into DAVID (<http://>

david.abcc.ncifcrf.gov/home.jsp), which revealed significant KEGG pathways presented in Figure 1D and a list of genes from cell cycle class presented in Figure 1E. This proliferative capacity of macrophages is consistent with that published recently^{12,13}. In these analyses we also found significant enrichment for immune function (Figure 1F, which will be discussed later) as well as a range of other functions which we placed under miscellaneous, Figure 1G. Thus, when comparing rM against pro-inflammatory macrophages, resolution-phase macrophages were significantly enriched for pathways involved in cell proliferation and to a lesser extent immune function.

We next asked what genes were differentially-expressed in rM but not in inflammatory (10mg zymosan) or naive macrophages. The objective was to determine whether rM possess a unique phenotype compared to other macrophage populations. In this analysis, an FDR of 0.05 and fold difference of 1.5 revealed 342 genes specifically up- and down-regulated (Figure 2A) in rM with a sample list presented in Figure 2B. Using the CLICK algorithm on Expander to detect significantly-enriched functional gene sets for rM versus naive and pro-inflammatory macrophages revealed 4 clusters. Cluster 1 (191 probesets, Figure 2C) possess enriched functional data sets that are significantly elevated and exclusive to rM, with genes primarily involved in the regulation of antigen processing and presentation of peptide or polysaccharide antigens via MHC-II (GO 0002504), immune system process (GO 0002376), response to stimuli (GO 0050896) and regulation of T cell activation (GO 0050863) for instance. A table of all functionally-enriched classes is shown in Figure 2D with a list of these genes shown in Figure 2E. Thus, from these analyses we conclude that rM cells possess all the biosynthetic machinery for antigen uptake, processing and presentation as well as chemoattraction and priming of T/B cells.

Omitting pro-inflammatory macrophage and directly comparing rM to naive macrophages (FDR 0.05 and fold difference of 1.5) revealed enrichment primarily for immune system process (GO: 0002376), antigen processing and presentation of peptide or polysaccharide antigen via MHC-II (GO: 0002504), immune response (GO: 0006955) and regulation of leukocyte activation (GO: 0002694), Figure S4A-D. From these data we reasoned that naive tissue macrophages must be enriched for genes that control cell cycling.

In cluster 2 (154 probesets, Figure 2F), genes were down-regulated in rM compared to inflammatory and naive macrophages. This cluster was enriched for genes involved in developmental processes (GO 0032502), embryonic development (GO 0009790), adenyly nucleotide binding (GO 0030554) and cytoskeletal protein binding (GO 0008092), for instance. A list of genes involved in developmental processes is shown in Figure 2H. Cluster 3 (39 probesets) and 4 (91 probesets) represent profiles of genes differentially expressed in rM cells (Figure S3A-B and Figure S3 C-D, respectively), but not possessing significant biological functional enrichment.

Further analysis of all 342 genes differentially expressed in the rM cells versus naive and pro-inflammatory macrophages using the MGI GO enrichment tool (VLAD) also identified enrichment of the GO biological processes antigen presentation (e.g. Cd74, H2-Aa, H2-Ab1, H2-DMA, H2-Eb1), immune system and developmental processes (list too extensive, see Table S3) as well as cell activation (e.g. Ccl5, Ccr2, Cd74, Tnfsf4). However, this analysis

identified that rMs were also enriched for genes involved in regulation of cell migration (e.g. Adam8, Ccl5, Ccr2, Fut8, Plcb1, Tnfsf4) and apoptosis (e.g. Ccl5, Cd74, Gstp1, Prmt2, Ski, Tnfsf4, Wfs1) (Table 1 and Table S3). From these data we therefore reasoned that naive tissue macrophages must be enriched for genes that control leukocyte differentiation and apoptosis.

Gene ontology and pathway Analysis of rMs

Figure 3 is the author's interpretation of key pathways that define rM based on expression levels (Figure 1B and Figure 2B, up-regulated) and functional enrichment (Figure 2C). Here, pathways significantly expressed in rM cells and central to antigen uptake and processing are highlighted in orange with proteins central to these pathways, but not significantly enriched in rM, presented in white. Green highlights chemokines and their receptors expressed/secreted by rM that trigger T/B cell chemoattraction or that facilitates lymphocyte expansion, differentiation and interaction with T cells.

PCR validation and comparisons of rM

We next carried out quantitative RT-PCR which confirmed original microarray findings. For instance, Figure 4A represents genes up-regulated in rM versus pro-inflammatory macrophages. Figure S5A-C further validates genes significantly up-regulated in rM versus naive and pro-inflammatory (panel A), while panel B-C highlight genes that are suppressed in rM compared to either pro-inflammatory macrophages (B) or naive and pro-inflammatory macrophages (C). In addition, data from these experiments confirmed the temporal profile of these genes enriched in rM, especially the biphasic expression of these genes in naive and again at resolution (Figure 4). Given the apparent dendritic cell-like phenotype deduced in Figure 3, we also included CD209a (monocytes-derived dendritic cell marker) in these analysis which was found to be significantly up-regulated in rM versus pro-inflammatory macrophages using both the microarray analysis (P value 0.0000167, data not shown) and quantitative RT-PCR (Figure 4B).

rM compared to conventional *in vitro*-derived M1 and M2 macrophages

While we previously found that rM have elevated iNOS and COX 2, markers typical of classically-activated M1 cells and thereby suggesting a hybrid phenotype⁸, we didn't make a direct comparison with *in vitro* M1/M2. Taking this further, we compared our *in vivo*-derived rM with *in vitro* M1 (LPS/INF γ) and M2 (IL-4) polarised BMDMs. Here, typical pro-inflammatory markers such as Nos2 (iNOS), Il12(p40), Tnfa, Il1b and Ptgs2 (COX 2) are expectedly higher in M1 than M2 BMDMs, but are differentially expressed in rM, Figure 4C. Similarly, typical M2 markers such as mannose receptor, Il10, Ym1, Fizz1, Arg1, mannose receptor (Mr) and Il1ra, while generally higher in alternatively-activated macrophages are also differentially expressed in resolution-phase rM cells, Figure 4D. We also find genes that have been previously shown to be enriched in M2b (regulatory macrophages) polarised using immune complexes (HbEGF, LIGHT and SPHK1)¹⁴ are also significantly up-regulated (Figure 4E). Thus, the results from these experiments prove that rM possess a unique phenotype inconsistent with conventional macrophage nomenclature, but most akin to M2b macrophages.

FACS profile of resolving peritonitis

In order to analyse the temporal profile of monocytes/macrophages throughout resolving inflammation, FACS analysis was conducted using the following markers: Ly6c (monocytes), F4/80 (macrophages) MHC-II, CD86 (antigen presentation/costimulatory marker), CD62L (lost on monocytes as they differentiate), CD11b and 7/4 antigen (Ag) (expressed on activated macrophages but not un-stimulated tissue histiocytes). In two of the time-points (naïve and 72h 0.1mg zymosan) we also characterised myeloid derived marker CD115 and C-lectin receptor CD209 (DC-SIGN). Thus, in the naive cavity Ly6c and F4/80 double labelling revealed two categories of monocytes/macrophages (Figure 5A) namely (i) Ly6c^{neg}F480^{int} (~2%) and (ii) Ly6c^{neg}F480^{hi} macrophages, the latter comprising ~40% of the total population. The remaining 60% of cells in the resting peritoneum comprise B1a/b, B2 and CD3-positive lymphocytes¹⁵ and very few CD11c^{pos} dendritic cells (~1% of total cells, see Figure S1C and D). Further characterisation reveals that the two macrophage populations differ in their size (data not shown) and expression of CD11b, MHC-II, CD86, CD115 and CD209 (Figure 5Ai and ii), which corroborates the findings of others¹⁶.

Ly6c^{hi}/F480^{int} and Ly6c^{hi}/F480^{hi} monocytes/macrophages were identified at 4h and 12h, respectively (Figure S6A [4h] and B [12h]) with only Ly6c^{hi}/F480^{hi} cells expressing MHC-II at 12h (Figure S6B). At 24h Ly6c^{hi}/F480^{hi} (Figure 5Bi) and Ly6c^{int}/F480^{hi} (Figure 5Bii) monocyte/macrophages were found with Ly6c^{int}/F480^{hi} cells expressing comparatively higher levels of MHC-II and CD11b. Greater numbers of Ly6c^{int}/F480^{hi} cells also expressed CD62L (Figure 5Bii).

By 48h three populations of monocyte/macrophages were identified including Ly6c^{hi}/F480^{int}, Ly6c^{int}/F480^{int} and Ly6c^{neg}/F480^{hi} (Figure 5Ci-iii, respectively) with CD11b and MHC-II expression increasing on cells upon their greater acquisition of F4/80. At 72h Ly6c^{hi}/F480^{int} and Ly6c^{neg}/F480^{hi} cells predominate with the latter mature macrophages expressing higher levels of CD11b, MHC-II and CD86, CD62L and CD209; both populations are CD11c negative, Figure 5Di-ii. 72h 10mg zymosan-inflamed cavity possessed Ly6c^{pos}/F480^{pos} and Ly6c^{neg}/F480^{pos} monocytes/macrophages that were MHC-II^{low} compared to resolution-phase macrophages, Figure 5Ei and ii.

PCR analysis of monocytes/macrophage sorted sub-population

Flow cytometry identified two categories of monocytes/macrophages that variably express F4/80 alone or F480/Ly6c over time. However, initial transcriptomic analysis was carried out on total monocytes/macrophage and the expression of key genes that defines rM in individual populations is unknown. Therefore, using FACS cell sorting we isolated Ly6c^{pos}F480^{hi} and Ly6c^{neg}F480^{hi} cells at 24h, 48h and 72h during resolving inflammation as well as Ly6c^{neg}F480^{hi} macrophages at 72h 10mg zymosan and quantified the expression of a number of genes enriched in rM (taken from Figure 1B and Figure 2) in each population using quantitative RT-PCR, Figure 6. Since each population is proportionally distinct and their population size varies over time we normalised gene expression to the percentage of each region at the specific time point. The rM specific markers including Cd86, H2Aa, Ccr2 and Ccl5, obtained from comparing rM against pro-inflammatory and naive macrophages (Figure 2) were highest in the Ly6c^{neg}F480^{hi} macrophage population. In addition, many of

the markers most elevated in rM compared to pro-inflammatory macrophages including Alox15, Tgfb2, Cxcl13 and Timd4 were also elevated in Ly6c^{neg}F480^{hi} macrophages as was the monocytes-derived DC marker CD209a, Figure 6.

Phenotype of rM compared to conventional dendritic cells

We compared key markers of rM cells to that expressed on splenic plasmacytoid and CD8 α ⁺/CD8 α ⁻ dendritic cells as well as GMCSF/IL-4 generated bone marrow-derived dendritic cells. CD11c was negative on macrophages from the naïve peritoneum as well as rM (Figure 7Ai and ii, respectively) but positive on bone marrow-derived dendritic cells (Figure 7Aiv) and expectedly FACS-sorted peritoneal CD11c-positive cells. The latter were not from the population of macrophages used for transcriptomic and PCR analysis, see Figure S1D. Furthermore, CD8^{pos}, CD8^{neg} and plasmacytoid dendritic cells were characterised as in Figure 7B and along with GMCSF/IL-4 generated bone marrow-derived dendritic cells were compared to rM at message level. Thus, MHC-II (Figure 5D) as well as co-stimulatory molecules (CD74 and CD86), monocyte-derived dendritic cells marker (CD209a) and the immune synapse mediator Clec2i are all expressed on rM cells albeit at variable levels compared to conventional dendritic cells, (Figure 7C).

Discussion

In this study we carried out mRNA transcriptomic analysis of macrophages present during the resolution of acute murine peritonitis revealing a phenotype inconsistent with the conventional M1/M2 nomenclature, but possessing aspects of all populations described so far. Uniquely, rM are primarily antigen processing and presenting with the ability to trigger T/B cell chemoattraction. rM are also positive for Tgfb2 and Alox15, the latter metabolises arachidonic (to HETEs and lipoxins)^{9,10}, eicosapentaenoic (to HEPES and resolvins)^{17–19} or docosahexaenoic acid (to docosatrienes, protectins and resolvins)^{18,20,21}. These are fatty acids implicated in anti-inflammatory and pro-resolution processes²². Also highly expressed in F4/80-positive rM and central to resolution is Timd4, a macrophage receptor that recognises phosphatidylserine expressed on apoptosing leukocytes¹¹. This divergence from the established M1/M2 paradigm has been reported elsewhere. For instance, in carbon-tetrachloride induced liver fibrosis two functionally distinct types of macrophages exist - during the injury phase the predominant macrophage phenotype is closest to that of M2, while during recovery from injury, macrophages are more M1-like²³. These authors suggest that the established M1/M2 model inadequately reflects the complex roles of these cells *in vivo* during liver injury. Indeed, in ischemically injured kidney, proximal tubule cells are proposed to regulate macrophage phenotype²⁴. Specifically, co-culturing proximal tubule cells with BMDMs induces a phenotype that has elevated IL-1 β and the macrophage scavenger receptor 1 (Msr1) but low levels of the M2 markers Ym1 or Igf1. However, these hybrid macrophages were associated with renal repair suggesting, again, that the M1/M2 paradigm needs re-addressing and that macrophage phenotype will vary depending on the tissue as well as the aetiology of the inflammatory response.

In the bone marrow, a common monocyte-DC precursor gives rise to monocytes and other precursors termed common DC precursors²⁵ and MHC-II/CD11c^{int} positive pre-cDCs²⁶.

Pre-cDCs move into the blood and from there, to lymphoid and nonlymphoid tissues forming CD11c^{hi}/MHC-II^{hi} DCs^{26,27}. Peripheral blood monocytes also differentiate *in vitro* into DCs (monocyte-derived DCs [Mo-DCs]) in the presence of GM-CSF/IL-4 acquiring dendritic morphology, losing the capacity to phagocytose and adhere to tissue culture surfaces^{28,29}. Several reports have documented the differentiation of murine CD11c^{neg} and MHC-II^{neg} blood monocytes into CD11c^{pos}MHC-II^{pos} Mo-DCs during various infectious and non-infectious stimuli^{30–32}. These Mo-DCs present protein antigens to TCR transgenic CD4^{pos} T cells and are distinguished from classical DCs by expression of the monocytes markers Gr-1/Ly6c. More recently, the *in vivo* differentiation of monocytes to DC-SIGN/CD209^{pos} Mo-DCs was demonstrated in response to LPS³³. These Mo-DCs lost expression of Gr-1/Ly6c and CD115/c-fms, upregulated TLR4 and CD14, acquired the probing morphology typical of DCs, localized to the T cell areas, and through Trif signalling become powerful antigen-capturing and -presenting cells, including cross-presentation of Gram-negative bacteria. In our studies we report that rM but not naive or pro-inflamed macrophages, are enriched with the biochemical machinery necessary for antigen processing and presentation (for example MHC-II [H2-Eb1, H2-Ab1, H2-Ob, H2-Aa], CD74, CD86), (2) secrete T- and B-lymphocyte chemokines (for example Xcl1, Ccl5, Cxcl13) and (3) secrete factors that enhance macrophage/dendritic cell development and promote DC/T cells synapse formation (for example Clec2i, Tnfsf4, Clec1). We also demonstrate that these cells express high levels of the Mo-DC marker, CD209a. Further FACS analysis of the macrophages during resolution displays 3 sub-populations present within the cavity (Ly6c^{pos}F4/80^{neg}, Ly6c^{neg}F4/80^{int} and Ly6c^{neg}F4/80^{hi}) that could contribute to the overall phenotype. We find that the Ly6c^{neg}F4/80^{hi} subset, which comprises of ~50% resident macrophages originally present in the naive, uninflamed cavity, selectively expresses both MHC-II and CD86 as inflammation resolves. In addition, it is these cells that increasingly express the T- and B-cell chemoattractants, Ccl5 and Cxcl3 and the C-lectin receptor, CD209a. Interestingly, we see a dramatic influx of T- (CD3^{pos}) and B-cells (CD19^{pos}) in to the resolving/post inflamed peritoneum from day 3 onwards (data not shown). It is therefore, likely that the role of rM and Ly6c^{neg}F4/80^{hi}, in particular, is in the generation of tissue memory lymphocytes. In addition, given the high levels of CD209a but paucity of CD11c expression on rM we concur with the finding of others that blood monocytes give rise to a macrophages with hallmarks of a DC in the peritoneum.

There are a series of sequential and often overlapping events collectively required to bring about resolution of acute inflammation and restore homeostasis^{34,35}. And while this is the prevailing view, data presented in this paper advances our understanding of resolution by suggesting that post-inflamed tissues do not readily revert back to their pre-inflamed/homeostatic state once PMNs disappear (arbitrary definition of inflammatory resolution). Instead, such tissues are populated for a number of weeks with macrophages possessing a unique resolution phenotype described here. In fact, we argue that the ultimate aim of effective resolution is required to fashion out macrophages that mediates tissue memory. Deviation may result in the generation of more M1-like, non-specific macrophages as in response to 10 mg zymosan. We are not aware of any other study that has drawn attention to rM as DC-like central players in the generation of tissue memory lymphocytes. And while we are aware that some conventional anti-inflammatory regimes maybe resolution toxic as

defined by prolonging PMN numbers³⁵, we are equally unaware of the impact nonsteroidal anti-inflammatory drugs, steroids or biologics, for instance, may unwittingly have on this aspect of the resolution cascade. We re-iterate that if the role of rM is to generate tissue memory against further infection/injury, perturbing this process could compromise the host's ability to mount appropriate secondary responses.

In contrast, mice injected with 10mg zymosan experienced a transient and aggressive, but nonetheless, resolving peritonitis. Isolation of macrophages from the peak of this hyper-inflamed state (72h) revealed a phenotype that was pro-inflammatory. Further investigations revealed that these macrophages did not acquire an rM phenotype once inflammation abated as defined by clearance of PMNs and cytokines, but maintained their distinctly pro-inflammatory state. While these findings provide an example of where macrophage phenotype remains rigid despite an apparent change in tissue pathology back to homeostasis, we cannot exclude the persistence/absence of a soluble mediator and/or cell type that drives and M1-like state. Thus, understanding the endogenous soluble mediators/cells types that lead to the failed acquisition of a pro-resolution phenotype in such an experimental model may provide opportunities for unravelling the phenotype of non-specific macrophages that occupy chronically-inflamed tissue such as alveolar macrophage from chronic obstructive pulmonary disease patients.

In summary, carrying out a full transcriptomic analysis of resolution-phase macrophage has revealed that these cells are enriched with the capacity to proliferate, secrete T/B cell chemoattractants, present antigens, as well as carry out more conventional aspects of resolution arising from the expression of Alox15 and its generation of pro-resolution lipoxins as well as Timd4, which is important in the phagocytosis of apoptotic cells. This repertoire of genes that control these diverse processes do not readily fall into the M1/M2 classification of macrophage phenotype, but are more regulatory and modulatory in nature.

Supplementary Material

Refer to Web version on PubMed Central for supplementary material.

Acknowledgements

DWG is a Wellcome Trust funded senior research fellow while MJS is a recipient of a Medical Research Council/GlaxoSmithKline-funded fellowship. The authors declare that there is no competing financial interest for the work presented in this submission. DWG and MS designed and carried out the research and wrote the paper along with JN and JB who contributed to the research. SS carried out bioinformatics while EC and RL carried out gene ontology studies. SF supplied essential experimental tools. DWG, MS and SS analysed data. A special thanks Mr Dominic Sparkes who assisted MS with some experimentation.

References

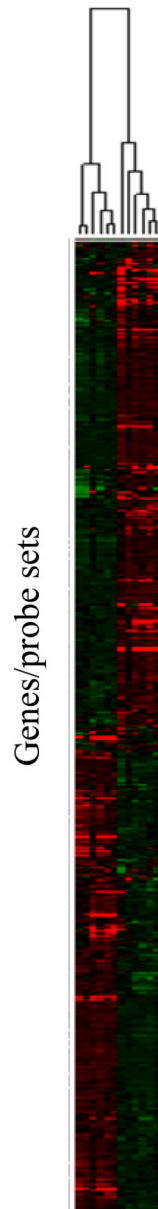
1. Bowdish DM, Loffredo MS, Mukhopadhyay S, Mantovani A, Gordon S. Macrophage receptors implicated in the "adaptive" form of innate immunity. *Microbes Infect.* 2007; 9(14-15):1680–1687. [PubMed: 18023392]
2. Savill J. Phagocyte recognition of apoptotic cells. *Biochem Soc Trans.* 1996; 24(4):1065–1069. [PubMed: 8968513]
3. van Furth R. Mycobacteria and macrophage activation. *Res Microbiol.* 1990; 141(2):256–261. [PubMed: 2111929]

4. Rosenthal AS, Lipsky PE, Shevach EM. Macrophage-lymphocyte interaction and antigen recognition. *Fed Proc.* 1975; 34(8):1743–1748. [PubMed: 1093892]
5. Shapiro SD. Diverse roles of macrophage matrix metalloproteinases in tissue destruction and tumor growth. *Thromb Haemost.* 1999; 82(2):846–849. [PubMed: 10605792]
6. Martinez FO, Sica A, Mantovani A, Locati M. Macrophage activation and polarization. *Front Biosci.* 2008; 13:453–461. [PubMed: 17981560]
7. Mosser DM, Edwards JP. Exploring the full spectrum of macrophage activation. *Nat Rev Immunol.* 2008; 8(12):958–969. [PubMed: 19029990]
8. Bystrom J, Evans I, Newson J, et al. Resolution-phase macrophages possess a unique inflammatory phenotype that is controlled by cAMP. *Blood.* 2008; 112(10):4117–4127. [PubMed: 18779392]
9. Serhan CN, Hamberg M, Samuelsson B. Lipoxins: novel series of biologically active compounds formed from arachidonic acid in human leukocytes. *Proc Natl Acad Sci U S A.* 1984; 81(17):5335–5339. [PubMed: 6089195]
10. Bannenberg GL, Aliberti J, Hong S, Sher A, Serhan C. Exogenous pathogen and plant 15-lipoxygenase initiate endogenous lipoxin A4 biosynthesis. *J Exp Med.* 2004; 199(4):515–523. [PubMed: 14970178]
11. Miyanishi M, Tada K, Koike M, Uchiyama Y, Kitamura T, Nagata S. Identification of Tim4 as a phosphatidylserine receptor. *Nature.* 2007; 450(7168):435–439. [PubMed: 17960135]
12. Jenkins SJ, Ruckerl D, Cook PC, et al. Local macrophage proliferation, rather than recruitment from the blood, is a signature of TH2 inflammation. *Science.* 2011; 332(6035):1284–1288. [PubMed: 21566158]
13. Davies LC, Rosas M, Smith PJ, Fraser DJ, Jones SA, Taylor PR. A quantifiable proliferative burst of tissue macrophages restores homeostatic macrophage populations after acute inflammation. *European journal of immunology.* 2011; 41(8):2155–2164. [PubMed: 21710478]
14. Edwards JP, Zhang X, Frauwirth KA, Mosser DM. Biochemical and functional characterization of three activated macrophage populations. *J Leukoc Biol.* 2006; 80(6):1298–1307. [PubMed: 16905575]
15. Rajakariar R, Lawrence T, Bystrom J, et al. Novel biphasic role for lymphocytes revealed during resolving inflammation. *Blood.* 2008; 111(8):4184–4192. [PubMed: 18218853]
16. Ghosn EE, Cassado AA, Govoni GR, et al. Two physically, functionally, and developmentally distinct peritoneal macrophage subsets. *Proc Natl Acad Sci U S A.* 2010; 107(6):2568–2573. [PubMed: 20133793]
17. Arita M, Bianchini F, Aliberti J, et al. Stereochemical assignment, antiinflammatory properties, and receptor for the omega-3 lipid mediator resolvin E1. *J Exp Med.* 2005; 201(5):713–722. [PubMed: 15753205]
18. Serhan CN, Hong S, Gronert K, et al. Resolvins: a family of bioactive products of omega-3 fatty acid transformation circuits initiated by aspirin treatment that counter proinflammation signals. *J Exp Med.* 2002; 196(8):1025–1037. [PubMed: 12391014]
19. Serhan CN, Clish CB, Brannon J, Colgan SP, Chiang N, Gronert K. Novel functional sets of lipid-derived mediators with antiinflammatory actions generated from omega-3 fatty acids via cyclooxygenase 2-nonsteroidal antiinflammatory drugs and transcellular processing. *J Exp Med.* 2000; 192(8):1197–1204. [PubMed: 11034610]
20. Hong S, Gronert K, Devchand PR, Moussignac RL, Serhan CN. Novel docosatrienes and 17S-resolvins generated from docosahexaenoic acid in murine brain, human blood, and glial cells. Autacoids in anti-inflammation. *J Biol Chem.* 2003; 278(17):14677–14687. [PubMed: 12590139]
21. Mukherjee PK, Marcheselli VL, Serhan CN, Bazan NG. Neuroprotectin D1: a docosahexaenoic acid-derived docosatriene protects human retinal pigment epithelial cells from oxidative stress. *Proc Natl Acad Sci U S A.* 2004; 101(22):8491–8496. [PubMed: 15152078]
22. Serhan CN, Chiang N. Endogenous pro-resolving and anti-inflammatory lipid mediators: a new pharmacologic genus. *Br J Pharmacol.* 2008; 153(Suppl 1):S200–215. [PubMed: 17965751]
23. Duffield JS, Forbes SJ, Constandinou CM, et al. Selective depletion of macrophages reveals distinct, opposing roles during liver injury and repair. *J Clin Invest.* 2005; 115(1):56–65. [PubMed: 15630444]

24. Lee S, Huen S, Nishio H, et al. Distinct macrophage phenotypes contribute to kidney injury and repair. *J Am Soc Nephrol*. 2011; 22(2):317–326. [PubMed: 21289217]
25. Naik SH, Sathe P, Park HY, et al. Development of plasmacytoid and conventional dendritic cell subtypes from single precursor cells derived in vitro and in vivo. *Nat Immunol*. 2007; 8(11):1217–1226. [PubMed: 17922015]
26. Liu K, Victora GD, Schwickert TA, et al. In vivo analysis of dendritic cell development and homeostasis. *Science*. 2009; 324(5925):392–397. [PubMed: 19286519]
27. Ginhoux F, Liu K, Helft J, et al. The origin and development of nonlymphoid tissue CD103+ DCs. *J Exp Med*. 2009; 206(13):3115–3130. [PubMed: 20008528]
28. Romani N, Gruner S, Brang D, et al. Proliferating dendritic cell progenitors in human blood. *J Exp Med*. 1994; 180(1):83–93. [PubMed: 8006603]
29. Sallusto F, Lanzavecchia A. Efficient presentation of soluble antigen by cultured human dendritic cells is maintained by granulocyte/macrophage colony-stimulating factor plus interleukin 4 and downregulated by tumor necrosis factor alpha. *J Exp Med*. 1994; 179(4):1109–1118. [PubMed: 8145033]
30. Leon B, Lopez-Bravo M, Ardavin C. Monocyte-derived dendritic cells formed at the infection site control the induction of protective T helper 1 responses against *Leishmania*. *Immunity*. 2007; 26(4):519–531. [PubMed: 17412618]
31. Serbina NV, Salazar-Mather TP, Biron CA, Kuziel WA, Pamer EG. TNF/iNOS-producing dendritic cells mediate innate immune defense against bacterial infection. *Immunity*. 2003; 19(1):59–70. [PubMed: 12871639]
32. Kool M, Soullie T, van Nimwegen M, et al. Alum adjuvant boosts adaptive immunity by inducing uric acid and activating inflammatory dendritic cells. *J Exp Med*. 2008; 205(4):869–882. [PubMed: 18362170]
33. Cheong C, Matos I, Choi JH, et al. Microbial stimulation fully differentiates monocytes to DC-SIGN/CD209(+) dendritic cells for immune T cell areas. *Cell*. 2010; 143(3):416–429. [PubMed: 21029863]
34. Gilroy DW, Feldmann M, Dabbagh K. Directed issue: novel concepts in inflammation. *Int J Biochem Cell Biol*. 2010; 42(4):480–481. [PubMed: 20149891]
35. Serhan CN, Brain SD, Buckley CD, et al. Resolution of inflammation: state of the art, definitions and terms. *FASEB J*. 2007; 21(2):325–332. [PubMed: 17267386]
36. Gentleman RC, Carey VJ, Bates DM, et al. Bioconductor: open software development for computational biology and bioinformatics. *Genome Biol*. 2004; 5(10):R80. [PubMed: 15461798]
37. Wu Z, Irizarry R, Gentleman R, Murillo FM, Spencer F. A Model-Based Background Adjustment for Oligonucleotide Expression Arrays. *Journal of the American Statistical Association*. 2004; 99:909–917.
38. Wilson CL, Miller CJ. Simpleaffy: a BioConductor package for Affymetrix Quality Control and data analysis. *Bioinformatics*. 2005; 21(18):3683–3685. [PubMed: 16076888]
39. Smyth GK. Linear models and empirical bayes methods for assessing differential expression in microarray experiments. *Stat Appl Genet Mol Biol*. 2004; 3 Article3.

A

72h 10mg 72h 0.1mg



B

Up-regulated

Rank	Gene Title (Gene Symbol)	Fold difference 0.1mg 72h vs 10mg 72h	Benjamini P Value
1	Arachidonate 15-lipoxygenase (Alox15)	8.2	3.48E-11
2	Guanylate nucleotide binding protein 1(Gpb1)	8.14	2.11E-09
3	Transforming growth factor beta 2 (Tgfb2)	8.03	1.62E-11
4	Latent transforming growth factor beta binding protein 1 (Ltbp1)	7.95	4.27E-10
5	Chemokine (C-X-C motif) ligand 13 (Cxcl13)	7.41	8.39E-07
6	Platelet selectin (Selp)	7.0	4.76E-10
7	Aspartocyclase (Aspa)	6.56	5.19E-10
8	Proteoglycan 4 (Prg4)	6.23	6.71E-12
9	GTPase activating RANGAP domain-like 3 (Garnl3)	6.21	1.82E-07
10	T-cell immun. & mucin domain containing 4 (Timd4)	6.09	5.28E-10
11	Coagulation factor V (F5)	6.02	2.21E-09
12	ST8 alpha-N-acetyl-neuraminide alpha-2,8-sialyltransferase 6 (St8sia6)	6.00	1.89E-10
13	Plexin domain containing 2 (Plxdc2)	5.74	1.13E-07
14	C-type lectin domain family 1, member a (Clec1a)	5.82	3.48E-09
15	Eph receptor A4 (Epha4)	5.4	2.47E-08
16	Endothelial cell selectin (Sele)	5.31	5.82E-09
17	Sulfotransferase family 1A, phenol-preferring, member 1 (Sult1a1)	5.26	3.83E-07
18	Ubiquitin-conjugating enzyme E2C (Ube2c)	5.18	4.68E-09
19	Cyclin B2 (Cnnb2)	5.12	1.93E-09
20	Shc SH2-domain binding protein 1 (Shcbp1)	4.94	8.93E-08

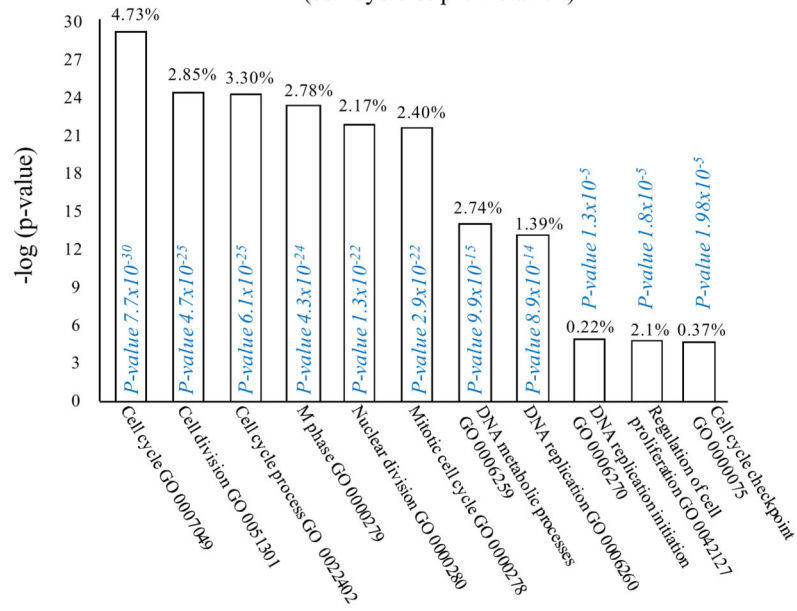
B

Down-regulated

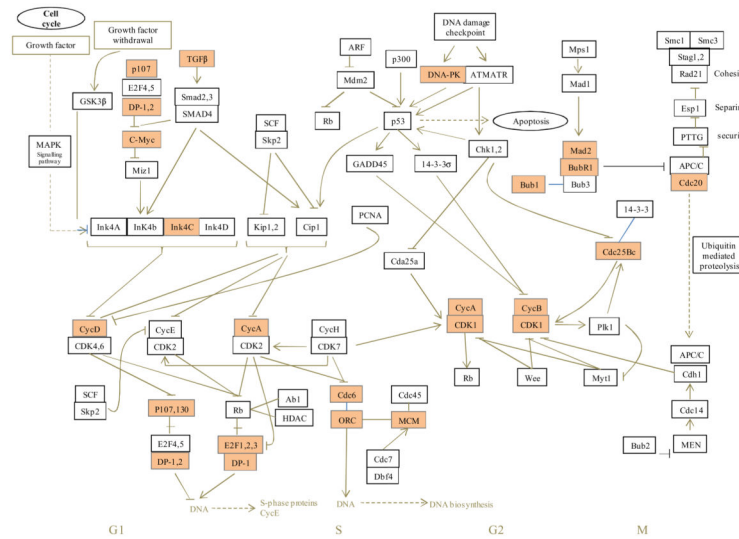
Rank	Gene Title (Gene Symbol)	Fold difference 0.1mg 72h vs 10mg 72h	Benjamini P Value
1	Glycoprotein (transmembrane) nmb (Gpnmb)	-8.43	7.51E-19
2	Stefin A2 like 1 (Stfa2l1)	-6.91	8.72E-08
3	AHNAK nucleoprotein 2 (Ahnak2)	-6.73	1.71E-14
4	Cathepsin K (Ctsk)	-6.34	3.57E-18
5	SPEG complex locus (Speg)	-6.27	4.25E-13
6	IL-1 family, Member 9 (Il1f9)	-6.1	2.60E-05
7	Family with sequence similarity 110, member C (Fam110c)	-5.96	1.64E-19
8	Tensin 1 (Tns1)	-5.84	1.55E-10
9	Aspartic peptidase (Asprv1)	-5.81	9.54E-08
10	Phosphatidic acid phosphatase type 2B (Ppap2b)	-5.6	6.39E-10
11	Solute carrier family 6 (Slc6a8)	-5.59	8.12E-16
12	Haemopoietic prostaglandin D synthase-2 (Hpgds)	-5.57	1.71E-10
13	ATPase, H ⁺ transporting, lysosomal (Atp6v0d2)	-5.53	5.15E-11
14	Tweety homolog 2 (Drosophila) (Ttyh2)	-5.49	9.16E-15
15	Membrane-spanning 4-domains, subfamily A, member 7 (Ms4a7)	-5.44	1.12E-11
16	Metalloprotease 8 (Mmp8)	-5.4	2.04E-13
17	Lipocalin 2 (Lcn2)	-5.39	6.10E-05
18	Aldo-keto reductase family 1, member B8 (Akr1b8)	-5.34	1.93E-14
19	Von Willebrand factor homolog (Vwf)	-5.24	2.54E-14
20	Matrix metalloproteinase 14 (membrane-inserted) (Mmp14)	-5.21	3.15E-10

C

Significantly enriched functional classes
(cell cycle & proliferation)



D



E

Probe ID	Gene Title	Gene Symbol	Fold difference 0.1mg 72h vs 10mg 72h	Benjamini P Value
[1419076_a_at]	Breast cancer 2	Brca2	1.8	5.61E-06
[1433873_s_at]	Pericentrin (Kendrin)	Pent	0.767	0.00168
[1448170_at]	Seven in absentia 2	Siah2	1.78	7.47E-08
[1452604_at]	stAR-related lipid transfer (START) domain containing 13	Stard13	1.05	0.0262
[1452606_at]	Meiotic nuclear division 1 homolog (S.cerivisae)	Mnd1	0.728	0.000852
[1440708_at]	Myosin, heavy polypeptide 9, non-muscle	Myh9	0.799	0.012
[1416988_at]	MutS homolog 2 (E.coli)	Msh2	1.19	0.000323
[1447932_at]	Zinc finger protein 830	Zfp830	1.08	0.000162
[1439376_x_at]	Cyclin D binding myb-like transcription factor 1	Dmtf1	0.898	0.00116
[1437370_at]	shugoshin-like (S.pombe)	Sgol2	1.28	0.00909
[1434079_s_at]	Minichromosome maintenance deficient 2 mitotin (S.cerivisae)	Mem2	1.42	2.30E-05
[1420029_at]	Minichromosome maintenance deficient 3 (S.cerivisae)	Mem3	0.774	0.000361
[1427462_at]	E2F transcription factor 3	E2f3	1.11	0.00028
[1431087_at]	SPC24, NDC80 kinetochore complex component, homolog (S.cerivisae)	Spc24	3.88	3.98E-07
[1433543_at]	Anillin, actin binding protein	Anln	2.91	5.40E-05
[1416251_at]	Minichromosome maintenance deficient 6 (Msi5 homolog, S. pombe)(S.cerivisae)	Mcm6	1.17	0.0081
[1417512_at]	Ectrophic viral integration site 5	Evi5	1.36	2.44E-06
[1436186_at]	E2F transcription factor 8	E2f8	1.3	0.0197
[1455730_at]	Discs, large (Drosophila) ho,olog-associated protein 5	Dlgap5	2.1	0.00548
[1434767_at]	Expressed sequence C79407	C79407	2.04	7.71E-05
[1420907_at]	CD2-associated protein	Cd2ap	0.678	0.00891
[1430811_a_at]	NUF2, NDC80 kinetochore complex component, homolog (S.cerivisae)	Nuf2	3.16	3.59E-05
[1417541_at]	Helicase, lymphoid specific	Hells	0.923	0.0334
[1427061_at]	Retinoblastoma binding protein 8	Rbbp8	0.799	0.00349
[1416757_at]	Zwilch, kinetochore associated homolog (Drosophila)	Zwilch	3.2	4.51E-06
[1430782_at]	Non-SMC condensin II complex, subunit D3	Ncapd3	1.31	0.00271
[1424143_a_at]	Chromatin licensing and DNA replication factor 1	Cdt1	0.73	0.0198
[1438173_x_at]	Polyamine-modulated factor 1	Pmf1	0.678	0.00057
[1428639_at]	Lin-9 homolog (C.elegans)	Lin9	1.32	0.00312
[1415849_s_at]	Stathmin 1	Stmn1	2.4	4.43E-08
[1423774_a_at]	Protein regulator of cytokinesis 1	Prc1	3.73	1.21E-06
[1452242_at]	Centrosomal protein 55	Cep55	4.57	2.90E-08
[1456477_at]	Cyclin T1	Cnt1	0.808	1.69E-05
[1416961_at]	Budding uninhibited by benzimidazoles 1 homolog, beta (S.cerivisae)	Bub1b	2.35	0.000797
[1444233_at]	G-protein coupled receptor 132	Gpr132	0.985	0.00576
[1437251_at]	Cell division cycle associated 2	Cdca2	4.32	8.46E-08
[1426897_at]	Regulator of chromosome condensation 2	Rcc2	1.3	0.0028
[1417019_a_at]	Cell division cycle 6 homolog (S.cerivisae)	Cdc6	1.02	0.00765
[1416802_a_at]	Cell division cycle associated 5	Cdca5	4.11	1.31E-07
[1424046_at]	Budding uninhibited by benzimidazoles 1 homolog (S.cerivisae)	Bub1	3.33	0.000123
[1426028_a_at]	Citron	Cit	2	0.000507
[1420639_at]	Junction-mediating and regulatory protein	Jmy	1.8	0.000679
[1427382_a_at]	Suppressor of variegation 3-9 homolog 1 (Drosophila)	Suv39h1	1.29	4.03E-05
[1429658_a_at]	Structural maintenance of chromosome 2	Smc2	2.28	1.07E-06
[1423920_at]	Non-SMC condensin I complex, subunit H	Ncaph	1.81	3.50E-05
[1418856_a_at]	Fanconi anemia, complementation, group A	Fanca	0.7795	0.0103
[1417445_at]	NDC80 homolog, kinetochore complex component (S.cerivisae)	Ndc80	3.43	8.40E-09
[1437580_s_at]	NIMA (never in mitosis gene a)-related expressed kinase 2	Nek2	1.11	0.000717
[1424511_at]	Aurora kinase A	Aurka	1.64	0.000112
[1437198_at]	Ligase III, DNA, ATP-dependent	Lig3	0.699	0.00321

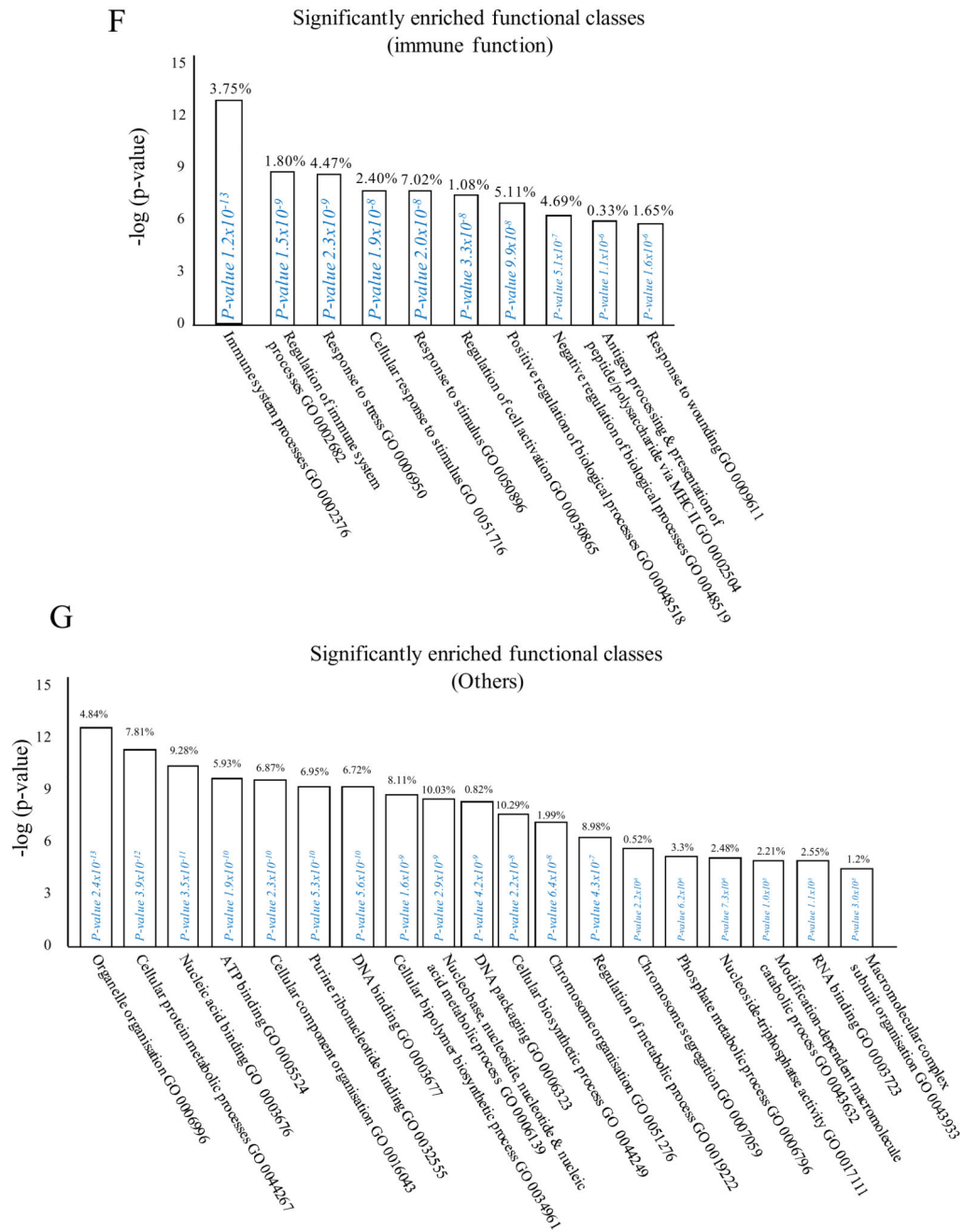
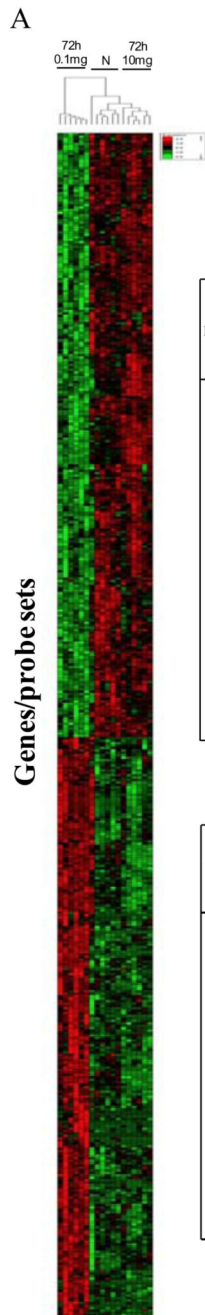


Figure 1. Phenotype of rM compared to pro-inflammatory macrophages.

In (A), gene expression of rM is compared to pro-inflammatory macrophages using cells from 6 animals showing a stark contrast in macrophage phenotypes while (B) reveals a sample of the top up- and down-regulated genes in rM cells versus pro-inflammatory macrophages based upon FDR of 0.05 and fold expression difference of 1.5. The software package Expander detected significantly enriched functional gene sets in rM versus pro-inflammatory macrophages including those for (C) proliferation with key genes enriched for cell cycling depicted in (D) and a list if these genes displayed in (E). In addition to

proliferation, other pathways were enriched in rM compared to pro-inflammatory macrophages namely (F) immune function and a range of other (G) significantly enriched functional classes.



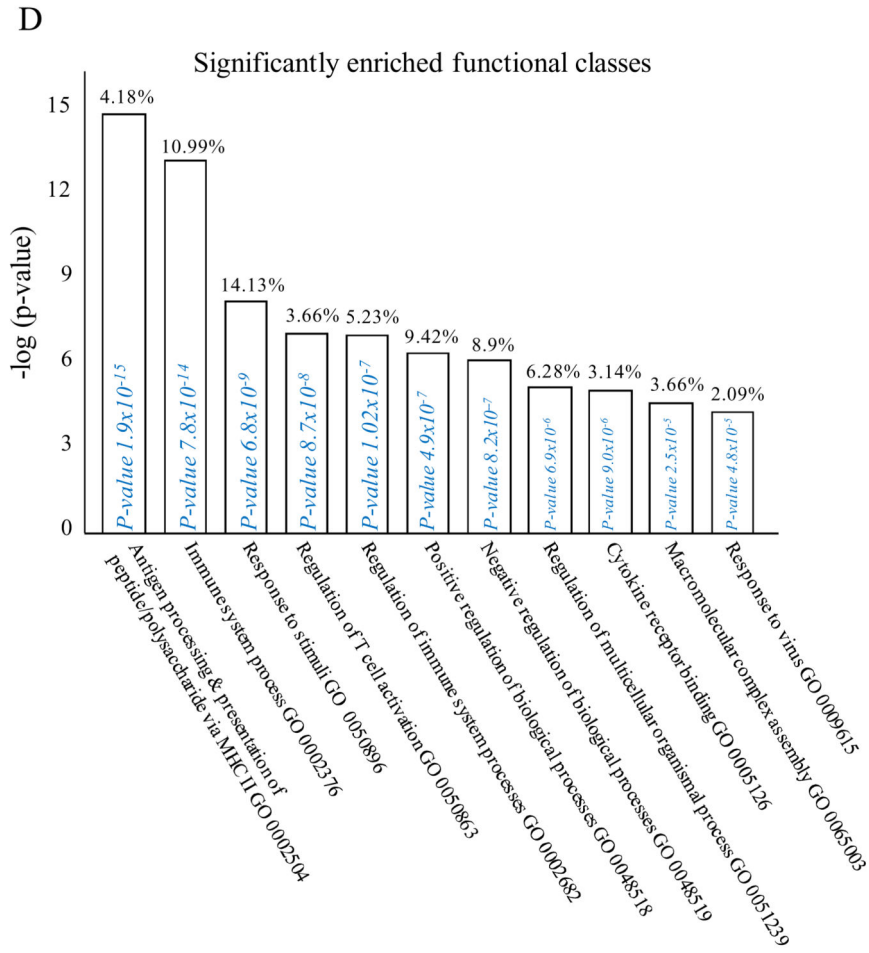
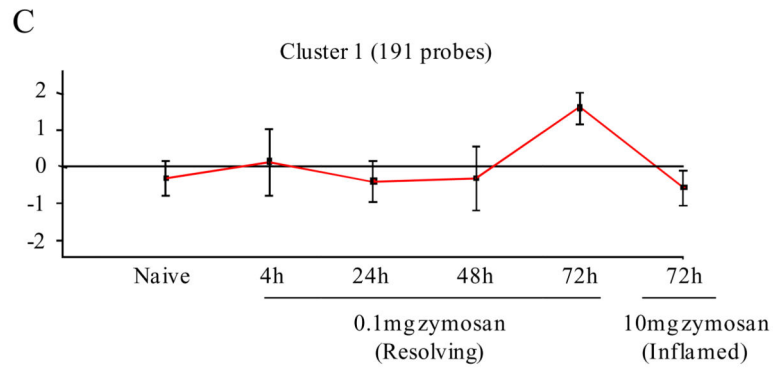
B

Up-regulated

Rank	Gene Title (Gene Symbol)	Fold difference 0.1mg 72h vs Naive	Benjamini P Value of 0.1mg 72h vs Naive	Fold difference 0.1mg 72h vs 10mg 72h	Benjamini P Value of 0.1mg 72h vs 10mg 72h
1	FtsJ homolog 2 (E. coli) (FtsJ2)	1.42	9.54E-05	2.85	2.81E-10
5	histocompatibility 2, class II antigen A, beta 1 (H2-Aβ1)	1.16	0.000232391	1.67	2.69E-07
7	histocompatibility 2, class II antigen A, alpha (H2-Aα)	2.39	2.53E-06	2.22	9.19E-07
8	CD74 antigen (invariant polypeptide of major histocompatibility complex, class II antigen-associated) (CD74)	1.44	0.000727106	1.95	3.73E-06
12	histocompatibility 2, class II antigen E beta (H2-Eβ)	1.64	0.000194102	1.83	9.22E-06
14	chemokine (C-C motif) receptor 2 (Ccr2)	3.24	1.65E-06	2.48	1.06E-05
15	calcium-binding tyrosine-(Y)-phosphorylation regulated (fibrousheathin 2) (Cabyr)	1.30	5.47E-05	1.27	1.35E-05
16	serine (or cysteine) peptidase inhibitor, clade B, member 6b (Serpinb6b)	1.49	4.12E-05	1.37	2.09E-05
18	glutathione S-transferase, pi 1 (Gstp1)	1.20	0.00073821	1.39	3.33E-05
19	histocompatibility 2, class II, locus Dma (H2-Dma)	2.43	0.000609413	2.75	3.38E-05
20	dihydropyrimidinase (Dpys)	1.62	0.000592208	1.80	3.92E-05
22	tumor necrosis factor (ligand) superfamily, member 4 (Tnfsf4)	3.46	6.39E-05	3.13	4.34E-05
27	histone cluster 1, H3f (Hist1h3f)	1.65	0.000435448	1.64	0.00011461
30	chemokine (C-C motif) ligand 5 (Ccl5)	2.22	0.000272417	1.96	0.000289544
33	membrane protein, palmitoylated 7 (MAGUK p55 subfamily member 7) (Mpp7)	1.14	0.000976655	1.12	0.000348477
54	kardiotropin-like cytokine factor 1 (Clefl1)	0.93	0.022835003	1.92	3.01E-06
67	chemokine (C-C motif) receptor 7 (Ccr7)	2.18	0.003494308	3.04	2.32E-05
86	C-type lectin domain family 2, member i (Clec2i)	1.48	0.007624318	1.97	0.000141644

Down-regulated

Rank	Gene Title (Gene Symbol)	Fold difference 0.1mg 72h vs Naive	Benjamini P Value of 0.1mg 72h vs Naive	Fold difference 0.1mg 72h vs 10mg 72h	Benjamini P Value of 0.1mg 72h vs 10mg 72h
1	α disintegrin and metallopeptidase domain 8 (Adam8)	-1.43	0.000147527	-2.11	9.45E-08
2	cathepsin L (Ctsl)	-1.05	0.00036078	-1.53	4.41E-07
3	mex3 homolog D (C. elegans) (Mex3d)	-1.13	0.000394162	-1.64	4.71E-07
4	ski sarcoma viral oncogene homolog (avian) (Ski)	-1.09	0.000288614	-1.55	4.80E-07
5	syntaxin binding protein 5 (tomosyn) (Stxbp5)	-2.18	2.15E-05	-2.42	7.32E-07
7	family with sequence similarity 114, member A1 (Fam114a1)	-1.62	0.000260539	-2.01	3.31E-06
8	serine/arginine-rich protein specific kinase 2 (Srpk2)	-1.08	0.000137736	-1.23	4.90E-06
10	lamin A (Lmna)	-1.13	0.000963234	-1.50	6.69E-06
12	heat shock 105kDa/110kDa protein 1 (Hsph1)	-2.30	6.30E-08	-1.37	2.09E-05
13	fukutin (Fktn)	-2.48	2.42E-07	-1.57	2.66E-05
14	tripartite motif-containing 32 (Trim32)	-1.43	0.000292561	-1.53	2.82E-05
16	Wolfram syndrome 1 homolog (human) (Wfs1)	-1.07	0.000689864	-1.20	4.40E-05
17	fucosyltransferase 8 (Fut8)	-2.31	9.36E-05	-1.97	0.000137806
18	xylulokinase homolog (H. influenzae) (Xylb)	-1.95	4.00E-06	-1.28	0.000171479
21	suppression of tumorigenicity 7-like (St7l)	-1.10	0.000586013	-1.04	0.000273388
22	protein arginine N-methyltransferase 2 (Prmt2)	-1.02	0.000990241	-1.02	0.000301509
24	heat shock protein 1 (Hspb1)	-1.67	0.000584788	-1.48	0.000584733
29	CD93 antigen (Cd93)	-0.80	0.006433705	-1.89	2.42E-08



E

Antigen processing and presentation of peptide/polysaccharide via MHC II GO 0002504

Probe ID	Gene Symbol	Gene Title	Fold difference 0.1mg 72h vs Naive	Benjamini P Value of 0.1mg 72h vs Naive	Fold difference 0.1mg 72h vs 10mg 72h	Benjamini P Value of 0.1mg 72h vs 10mg 72h
[1425519_a_at]	Cd74	CD74 antigen (invariant polypeptide of major histocompatibility complex, class II antigen-associated)	1.44	0.000727106	1.95	3.73E-06
[1452432_s_at]	H2-Aa	histocompatibility 2, class II antigen A, alpha	2.39	2.53E-06	2.22	9.19E-07
[1450648_s_at]	H2-Ab1	histocompatibility 2, class II antigen A, beta 1	1.16	0.000232391	1.67	2.69E-07
[1459872_x_at]	H2-DMa	histocompatibility 2, class II, locus Dma	2.43	0.000609413	2.75	3.38E-05
[1418638_at]	----	----	1.89	0.000169756	1.79	6.58E-05
[1422201_at]	H2-Ob	histocompatibility 2, O region beta locus	1.13	0.011035407	1.31	0.001182414
[1417025_at]	H2-Eb1	histocompatibility 2, class II antigen E beta	1.64	0.000194102	1.83	9.22E-06
[1419297_at]	H2-Oa	histocompatibility 2, O region alpha locus	0.89	0.038164919	0.81	0.036489949

Immune system process GO 0002376

Probe ID	Gene Symbol	Gene Title	Fold difference 0.1mg 72h vs Naive	Benjamini P Value of 0.1mg 72h vs Naive	Fold difference 0.1mg 72h vs 10mg 72h	Benjamini P Value of 0.1mg 72h vs 10mg 72h
[1419412_at]	Xcl1	chemokine (C motif) ligand 1	2.58	0.000964	1.88	0.00609508
[1421744_at]	Tnfsf4	tumor necrosis factor (ligand) superfamily, member 4	3.46	6.39E-05	3.13	4.34E-05
[1452431_s_at]	H2-Aa	histocompatibility 2, class II antigen A, alpha	2.39	2.53E-06	2.22	9.19E-07
[1425519_a_at]	Cd74	CD74 antigen (invariant polypeptide of major histocompatibility complex, class II antigen-associated)	1.44	0.0007271	1.95	3.73E-06
[1450495_a_at]	Klrl1	killer cell lectin-like receptor subfamily K, member 1	1.26	0.0051028	1.45	0.00045467
[1450648_s_at]	H2-Ab1	histocompatibility 2, class II antigen A, beta 1	1.16	0.0002324	1.67	2.69E-07
[1427216_at]	Ifnz	interferon zeta	0.76	0.0253541	0.82	0.00654538
[1417025_at]	H2-Eb1	histocompatibility 2, class II antigen E beta	1.64	0.0001941	1.83	9.22E-06
[1423466_at]	Ccr7	chemokine (C-C motif) receptor 7	2.18	0.0034943	3.04	2.32E-05
[1439145_at]	Lck	lymphocyte protein tyrosine kinase	1.07	0.0277064	1.24	0.00407234
[1429563_x_at]	----	----	1.02	0.0215069	1.05	0.00826687
[1418126_at]	Ccl5	chemokine (C-C motif) ligand 5	2.22	0.0002724	1.96	0.00028954
[1437270_a_at]	Clefl	cardiotrophin-like cytokine factor 1	0.93	0.022835	1.92	3.01E-06
[1425947_at]	Ifng	interferon gamma	1.51	0.0056321	1.59	0.00133445
[1426276_at]	Ifih1	interferon induced with helicase C domain 1	0.91	0.0002031	0.99	1.55E-05
[1459872_x_at]	H2-DMa	histocompatibility 2, class II, locus Dma	2.43	0.0006094	2.75	3.38E-05
[1418638_at]	----	----	1.89	0.0001698	1.79	6.58E-05
[1422201_at]	H2-Ob	histocompatibility 2, O region beta locus	1.13	0.0110354	1.31	0.00118241
[1421065_at]	Jak2	Janus kinase 2	0.91	0.0035865	0.75	0.00703682
[1456426_at]	Clec2i	C-type lectin domain family 2, member i	1.48	0.0076243	1.97	0.00014164
[1419297_at]	H2-Oa	histocompatibility 2, O region alpha locus	0.89	0.0381649	0.81	0.03648995

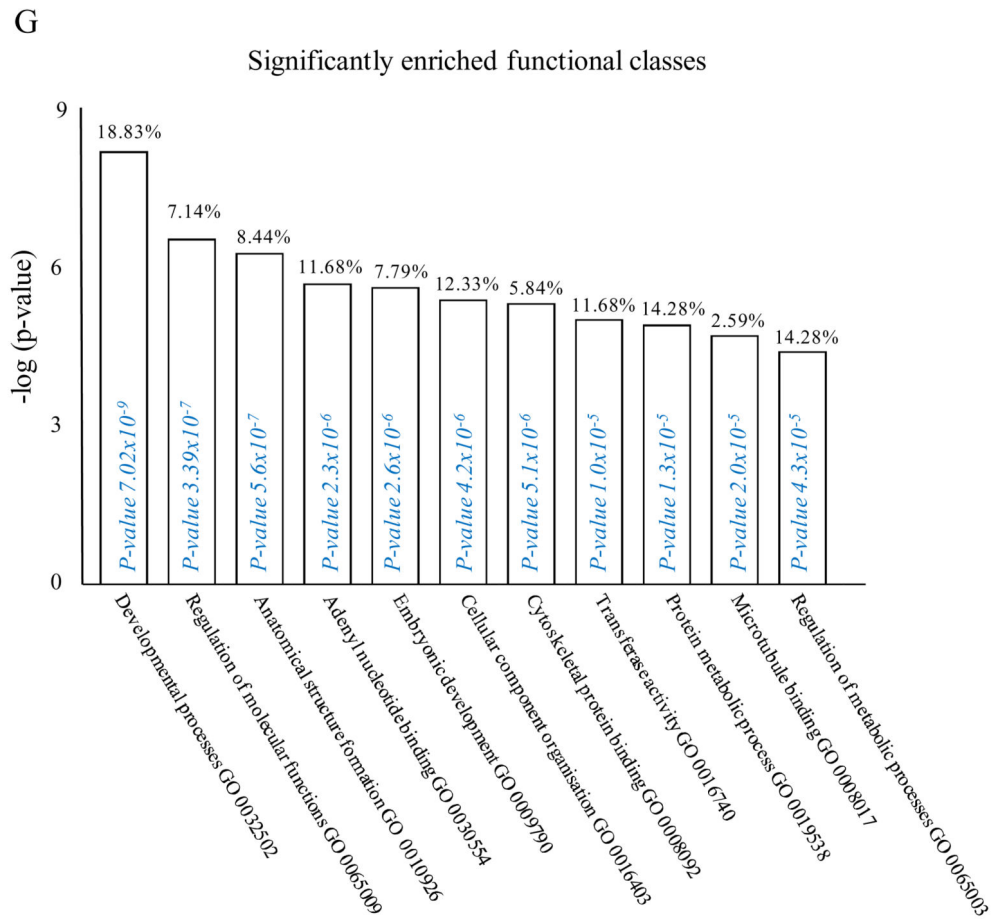
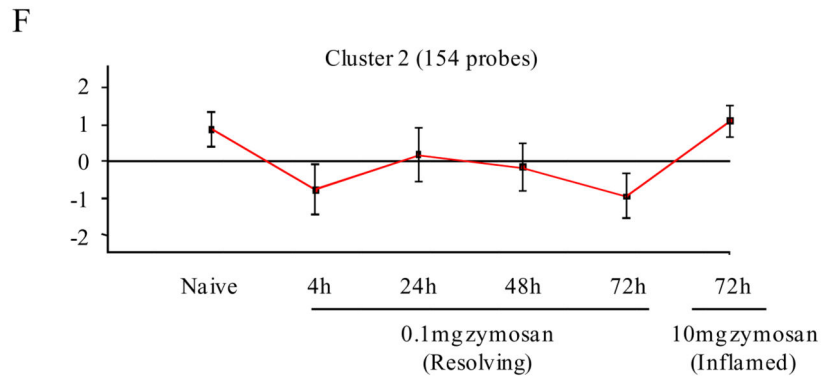
E

Response to stimuli GO 0050896

Probe ID	Gene Symbol	Gene Title	Fold difference 0.1mg 72h vs Naive	Benjamini P Value of 0.1mg 72h vs Naive	Fold difference 0.1mg 72h vs 10mg 72h	Benjamini P Value of 0.1mg 72h vs 10mg 72h
[1431591_s_at]	----	----	1.21	0.0166257	1.12	0.01340436
[1425519_a_at]	Cd74	CD74 antigen (invariant polypeptide of major histocompatibility complex, class II antigen-associated)	1.44	0.0007271	1.95	3.73E-06
[1458385_at]	Hspa41	heat shock protein 4 like	0.75	0.0388836	1.17	0.0003504
[1429563_x_at]	----	----	1.02	0.0215069	1.05	0.00826687
[1418126_at]	Ccl5	chemokine (C-C motif) ligand 5	2.22	0.0002724	1.96	0.00028954
[1425947_at]	Ifng	interferon gamma	1.51	0.0056321	1.59	0.00133445
[1419480_at]	Sell	selectin, lymphocyte	1.39	0.007502	1.52	0.00131539
[1459872_x_at]	H2-DMa	histocompatibility 2, class II, locus Dma	2.43	0.0006094	2.75	3.38E-05
[1418638_at]	----	----	1.89	0.0001698	1.79	6.58E-05
[1451596_a_at]	Sphk1	sphingosine kinase 1	1.21	0.001462	1.15	0.00073548
[1421407_at]	F2r12	coagulation factor II (thrombin) receptor-like 2	0.86	0.0154171	0.85	0.00739984
[1451928_a_at]	Rad18	RAD18 homolog (<i>S. cerevisiae</i>)	1.04	0.0034943	1.50	1.42E-05
[1418856_a_at]	Fanca	Fanconi anemia, complementation group A	0.94	0.006422	0.80	0.01027781
[1423877_at]	Chaf1b	chromatin assembly factor 1, subunit B (p60)	1.45	0.0072792	2.68	1.59E-06
[1421744_at]	Tnfr4	tumor necrosis factor (ligand) superfamily, member 4	3.46	6.39E-05	3.13	4.34E-05
[1419412_at]	Xcl1	chemokine (C motif) ligand 1	2.58	0.000964	1.88	0.00609508
[1452431_s_at]	H2-Aa	histocompatibility 2, class II antigen A, alpha	2.39	2.53E-06	2.22	9.19E-07
[1450648_s_at]	H2-Ab1	histocompatibility 2, class II antigen A, beta 1	1.16	0.0002324	1.67	2.69E-07
[1422567_at]	Fam129a	family with sequence similarity 129, member A	1.05	0.0009899	0.89	0.00153816
[1423466_at]	Ccr7	chemokine (C-C motif) receptor 7	2.18	0.0034943	3.04	2.32E-05
[1417025_at]	H2-Eb1	histocompatibility 2, class II antigen E beta	1.64	0.0001941	1.83	9.22E-06
[1427216_at]	Ifnz	interferon zeta	0.76	0.0253541	0.82	0.00654538
[1426276_at]	Ifih1	interferon induced with helicase C domain 1	0.91	0.0002031	0.99	1.55E-05
[1420931_at]	Mapk8	mitogen-activated protein kinase 8	0.98	0.0005091	0.67	0.00623511
[1422201_at]	H2-Ob	histocompatibility 2, O region beta locus	1.13	0.0110354	1.31	0.00118241
[1448314_at]	Cdk1	cyclin-dependent kinase 1	1.83	0.0126581	3.48	2.89E-06
[1421065_at]	Jak2	Janus kinase 2	0.91	0.0035865	0.75	0.00703682

Regulation of T cell activation GO 0050863

Probe ID	Gene Symbol	Gene Title	Fold difference 0.1mg 72h vs Naive	Benjamini P Value of 0.1mg 72h vs Naive	Fold difference 0.1mg 72h vs 10mg 72h	Benjamini P Value of 0.1mg 72h vs 10mg 72h
[1439145_at]	Lck	lymphocyte protein tyrosine kinase	1.07	0.0277064	1.24	0.00407234
[1425519_a_at]	Cd74	CD74 antigen (invariant polypeptide of major histocompatibility complex, class II antigen-associated)	1.44	0.0007271	1.95	3.73E-06
[1425947_at]	Ifng	interferon gamma	1.51	0.0056321	1.59	0.00133445
[1452431_s_at]	H2-Aa	histocompatibility 2, class II antigen A, alpha	2.39	2.53E-06	2.22	9.19E-07
[1459872_x_at]	H2-DMa	histocompatibility 2, class II, locus Dma	2.43	0.0006094	2.75	3.38E-05
[1456426_at]	Clec2i	C-type lectin domain family 2, member i	1.48	0.0076243	1.97	0.00014164
[1419297_at]	H2-Oa	histocompatibility 2, O region alpha locus	0.89	0.0381649	0.81	0.03648995



H

Developmental process GO 0032502

Probe ID	Gene Symbol	Gene Title	Fold difference 0.1mg 72h vs Naive	Benjamini P Value of 0.1mg 72h vs Naive	Fold difference 0.1mg 72h vs 10mg 72h	Benjamini P Value of 0.1mg 72h vs 10mg 72h
[1420977_at]	Man1a2	mannosidase, alpha, class 1A, member 2	-0.79	0.000406891	-0.64	0.001161095
[1452874_at]	2510003E04Rik	RIKEN cDNA 2510003E04 gene	-1.38	0.000335411	-1.57	1.44E-05
[1449941_at]	Myo1e	myosin IE	-1.56	0.042256644	-2.55	0.000253378
[1451200_at]	Kif1b	kinesin family member 1B	-0.61	0.02509788	-1.31	2.15E-06
[1449935_a_at]	Dnaj3	DnaJ (Hsp40) homolog, subfamily A, member 3	-0.81	0.002957842	-1.32	2.15E-06
[1424155_at]	Fabp4	fatty acid binding protein 4, adipocyte	-3.83	4.32E-09	-1.04	0.015082873
[1417783_at]	Als2	amyotrophic lateral sclerosis 2 (juvenile) homolog (human)	-1.37	0.027455728	-1.22	0.028842204
[1439582_at]	Macf1	microtubule-actin crosslinking factor 1	-1.84	0.000194102	-1.26	0.002728778
[1440799_s_at]	Farp2	FERM, RhoGEF and pleckstrin domain protein 2	-1.12	0.017511592	-1.16	0.005889969
[1426230_at]	Sphk2	sphingosine kinase 2	-2.83	3.56E-06	-1.04	0.030565038
[1429055_at]	4930506M07Rik	RIKEN cDNA 4930506M07 gene	-1.05	4.00E-05	-0.96	2.32E-05
[1460324_at]	Dnmt3a	DNA methyltransferase 3A	-1.25	0.002871983	-1.81	1.03E-05
[1417134_at]	Srpk2	serine/arginine-rich protein specific kinase 2	-0.94	0.004872143	-1.38	1.94E-05
[1443881_at]	Pofut1	protein O-fucosyltransferase 1	-0.93	0.001205552	-0.81	0.001598657
[1434557_at]	Hip1	huntingtin interacting protein 1	-0.96	3.24E-05	-0.82	4.94E-05
[1439619_at]	Tcf12	transcription factor 12	-1.61	0.00129491	-1.40	0.0016392
[1417846_at]	Ulk2	Unc-51 like kinase 2 (C. elegans)	-0.97	0.036967442	-1.21	0.003390129
[1426373_at]	Ski	ski sarcoma viral oncogene homolog (avian)	-1.09	0.000288614	-1.55	4.80E-07
[1423785_at]	Egln1	EGL nine homolog 1 (C. elegans)	-0.66	0.006064247	-0.86	0.000121568
[1417865_at]	Tnfaip1	tumor necrosis factor, alpha-induced protein 1 (endothelial)	-0.67	0.002745775	-0.64	0.001499315
[1448131_at]	Mfn2	mitofusin 2	-0.64	0.007510004	-0.76	0.000521238
[1419915_at]	Nus1	nuclear undecaprenyl pyrophosphate synthase 1 homolog (S. cerevisiae)	-0.93	5.58E-05	-0.64	0.001010169
[1448529_at]	Thbd	thrombomodulin	-1.53	0.001094226	-1.49	0.000434102
[1450716_at]	Adams1	a disintegrin-like and metallopeptidase (repolysin type) with thrombospondin type 1 motif, 1	-2.18	0.021709379	-1.79	0.037865083
[1447693_s_at]	Neo1	neogenin	-1.87	0.00824467	-1.78	0.005080741
[1417565_at]	Abhd5	abhydrolase domain containing 5	-0.74	0.00072538	-0.81	6.25E-05
[1436476_at]	Dand5	DAN domain family, member 5	-0.76	0.021412552	-0.75	0.010643655
[1451716_at]	Mafb	v-maf musculoaponeurotic fibrosarcoma oncogene family, protein B (avian)	-1.12	1.89E-05	-0.63	0.003026402
[1436051_at]	Myo5a	myosin VA	-0.91	0.022116155	-1.17	0.001176857

Figure 2. Genes enriched in rM cells compared to naive and pro-inflammatory macrophages. An FDR of 0.05 and fold difference of 1.5 revealed (A) 342 genes up- and down-regulated in rM compared to pro-inflammatory (10mg zymosan) and naive macrophages, a sample of the most differentially expressed genes is presented in (B). The software package Expander detected (C) 191 probesets significantly up-regulated in rM cells with these gene sets enriched for (D) aspect of antigen uptake/presentation and immune function with a list of the genes involved in antigen processing and presentation of peptide/polysaccharide via MHC-II (GO 0002504), immune system process (GO 0002376), response to stimuli (GO 0050896) and regulation of T cell activation (GO 0050863) shown in (E). There was significant enrichment for (F) 154 down regulated probesets with their significantly enriched functional classes presented in (G). Genes involved in developmental processes (GO 0032502) are listed in (H).

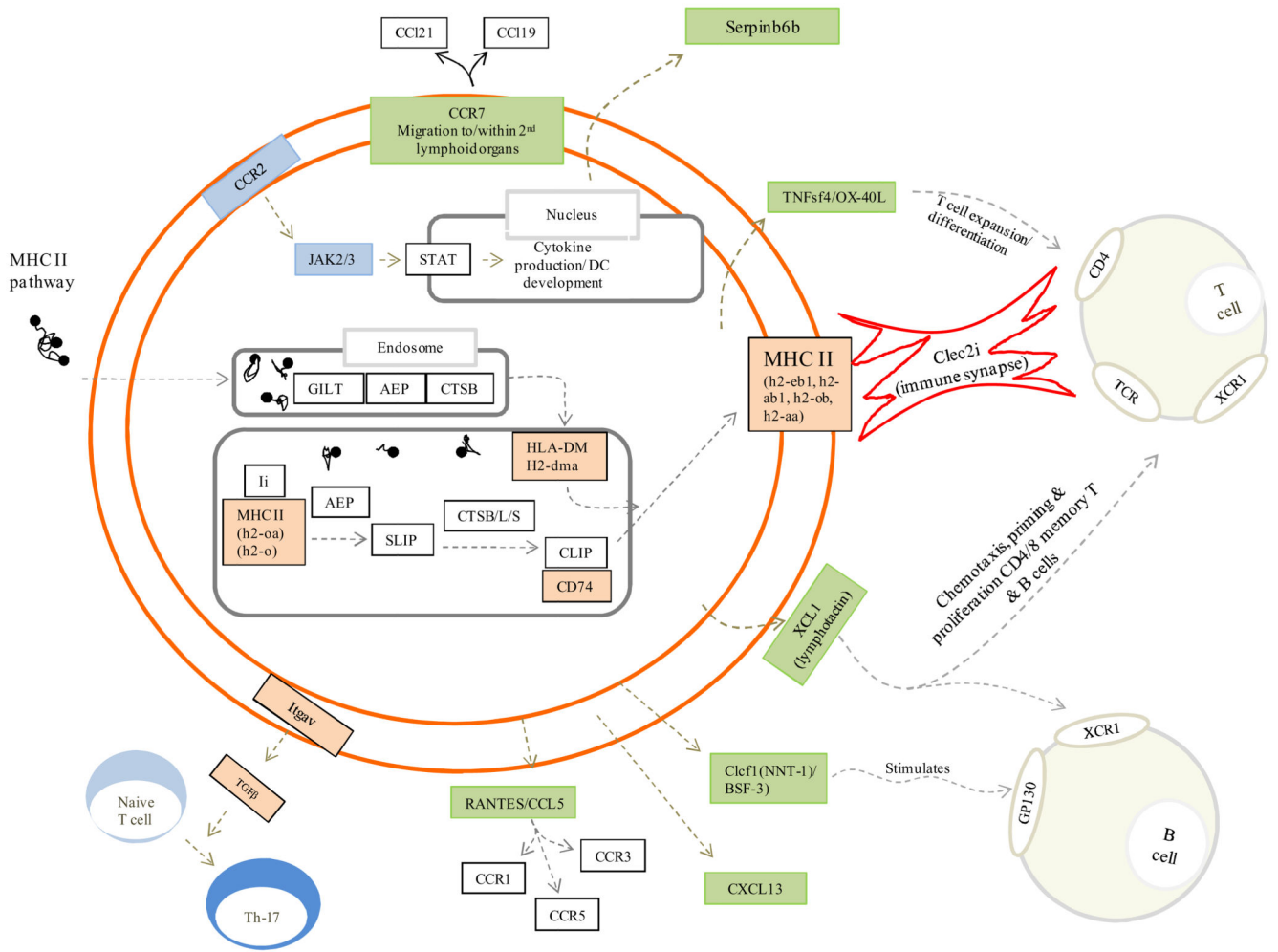
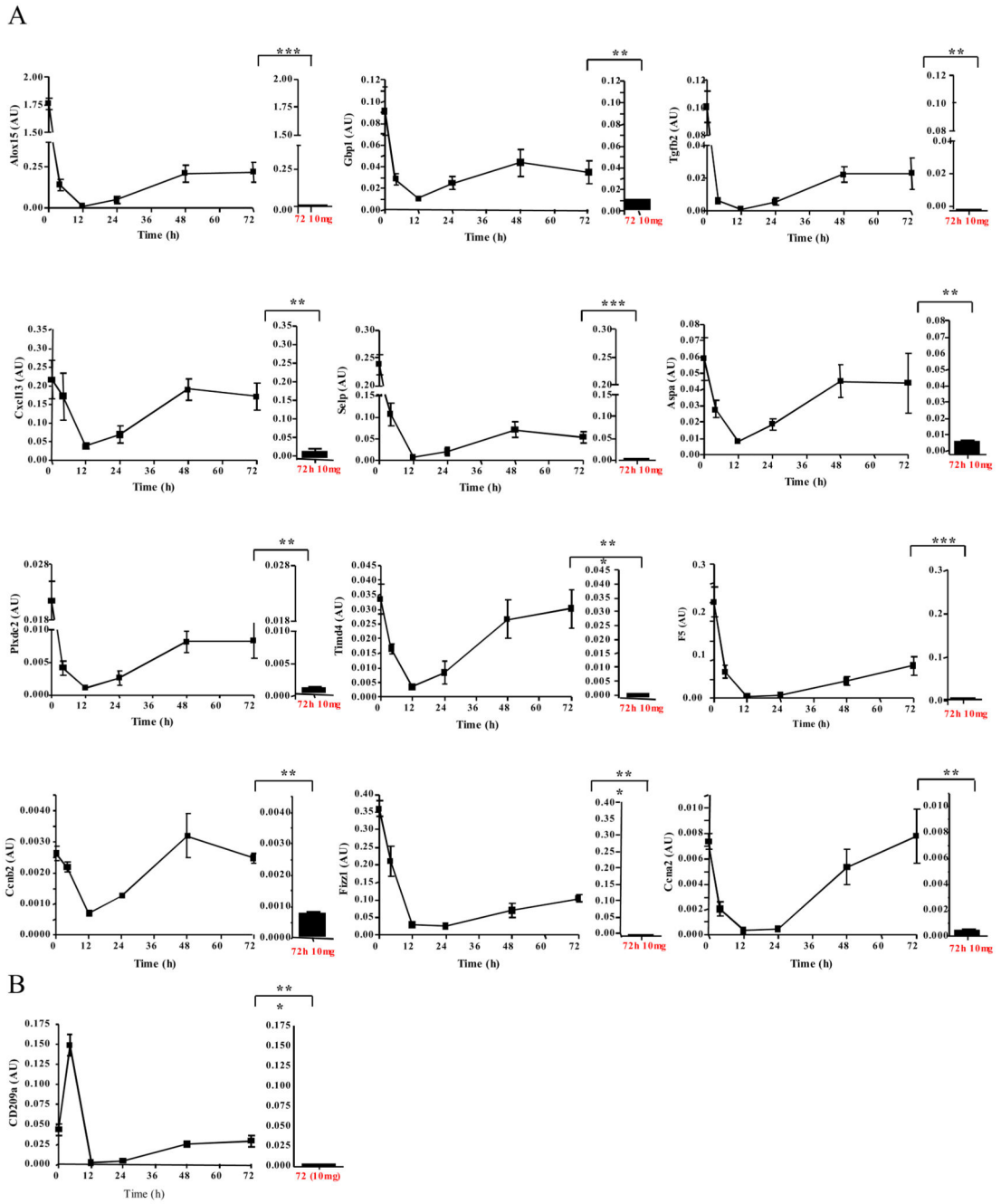


Figure 3. Unique phenotype of rM.

Author's interpretation of key pathways defining rM are highlighted in colour. In gold, for example, are those genes central to antigen uptake and processing (all other genes in this pathway are in white and not enriched in rM) while green highlights chemokines and their receptors expressed/secreted by rM that trigger T/B cell chemoattraction or that which facilitate lymphocyte expansion/differentiation or T cell/rM interaction such as Clec2i, TNFsF4/OX and XCL1.



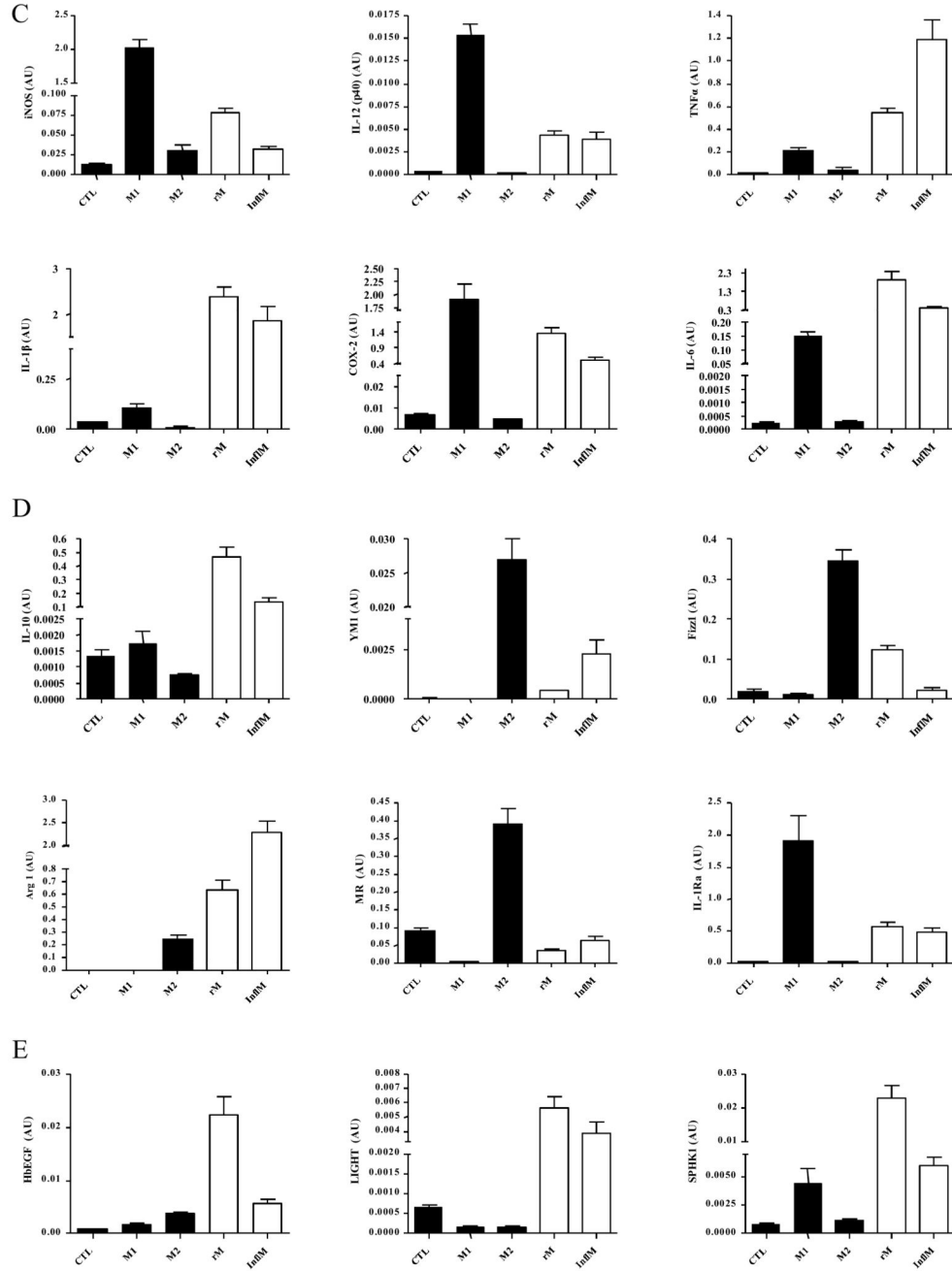
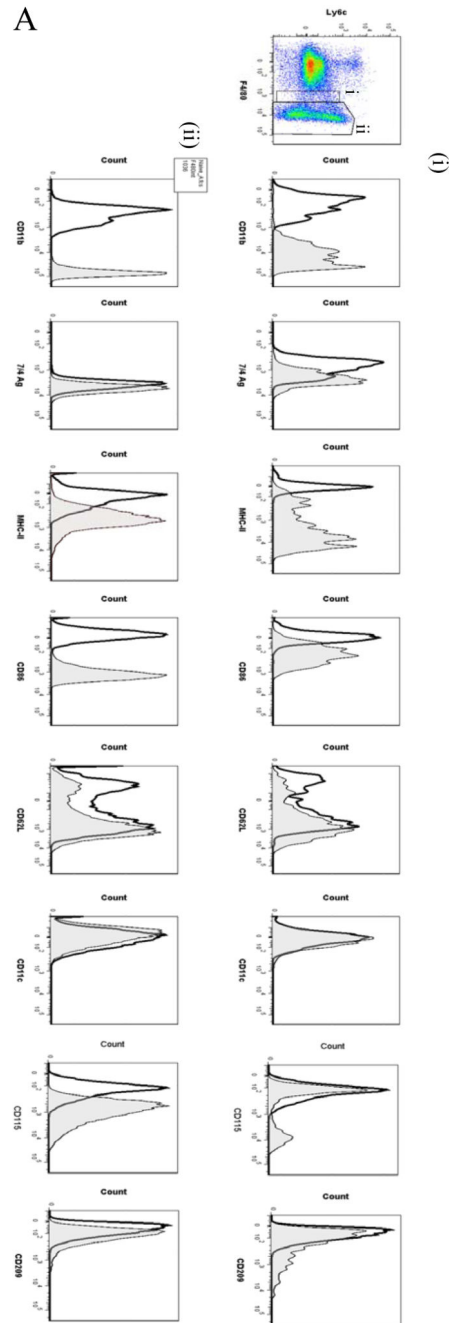
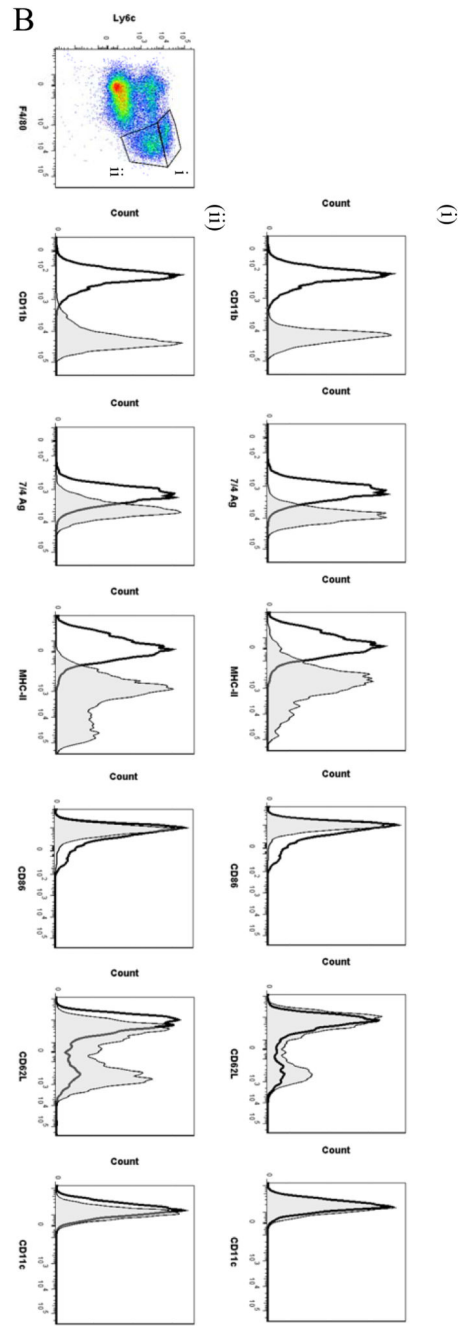


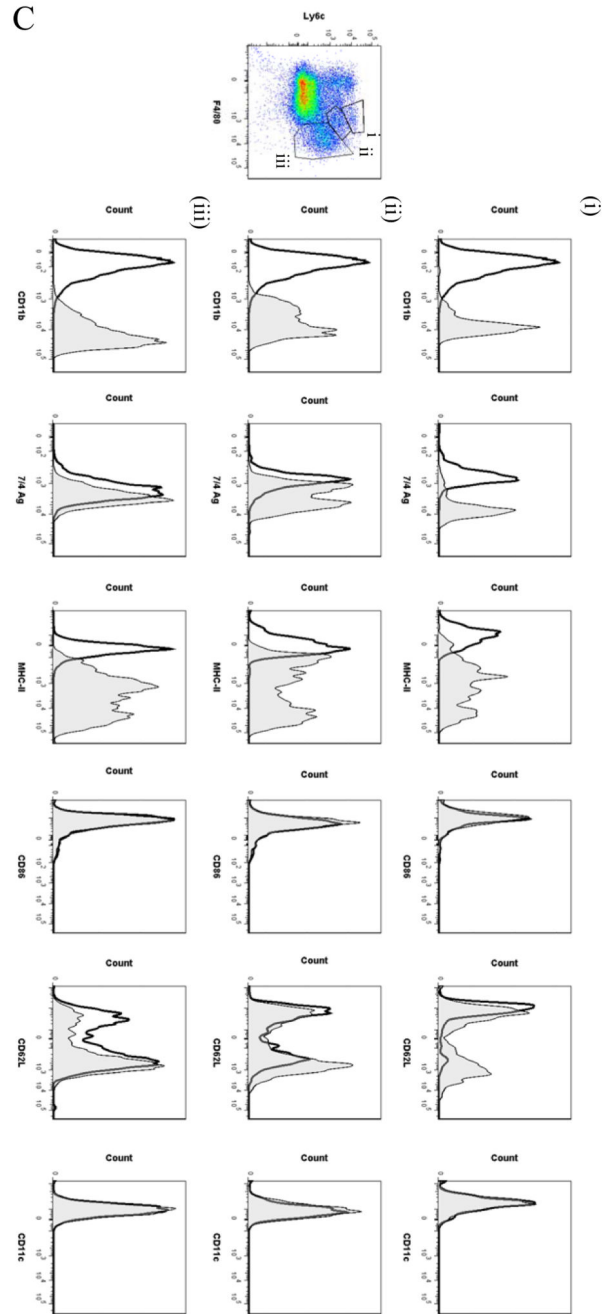
Figure 4. Validation of microarray analyses and phenotype of rM compared to *in vitro*-derived M1 and M2 macrophages.

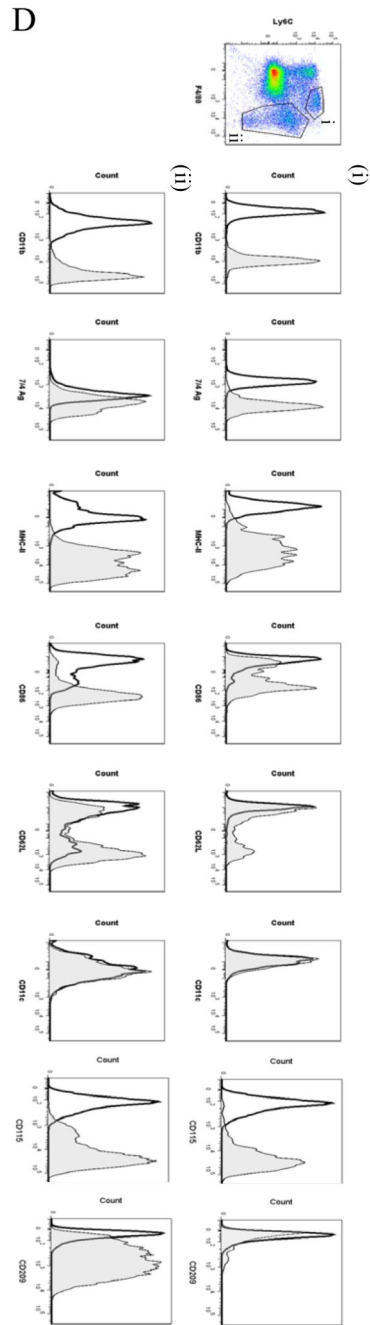
Quantitative PCR for (A) genes most differentially expressed in rM versus pro-inflammatory macrophages validating original microarray findings including (B) CD209a, the monocytes-derive DC marker, which was included arising from the DC-like phenotype deduced in Figure 3. For comparisons to established M1/M2 cells, BMDMs were incubated with either LPS/INF γ (M1) and or IL-4 (M2) for 24h. RNA was extracted and probed for a range of typical (C) M1, (D) M2, and (E) M2b markers. Data are represented and analysed by

ANOVA followed by Bonferroni multiple comparison tests. Values are expressed as means \pm SEM of n=5-6 mice per group. ** *P* value < 0.01 and *** *P* value < 0.001.









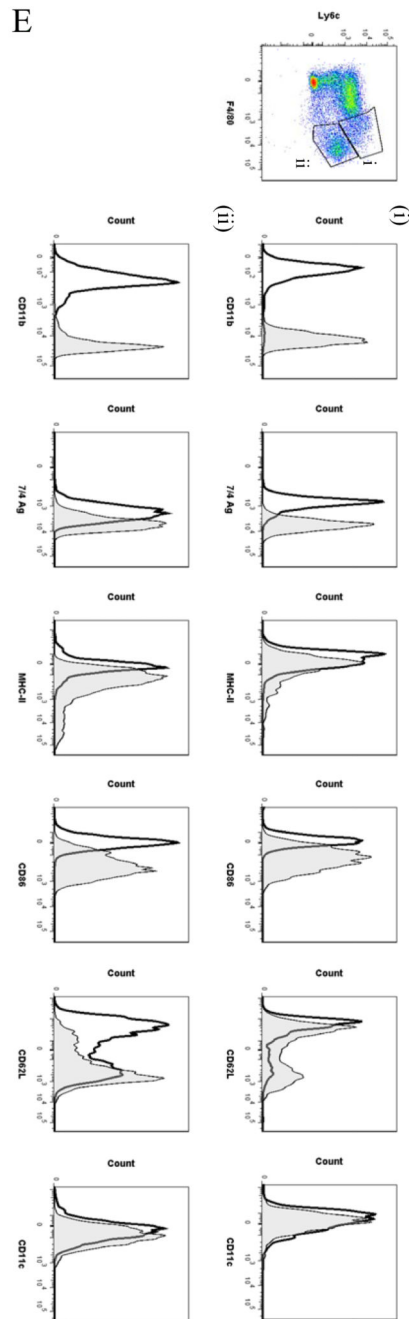


Figure 5. Temporal profile of monocytes and monocyte-derived macrophages during resolving inflammation.

Cells from the (A) naive peritoneum were labelled with Ly6c and F4/80, which identified two regions (i-ii) by FACS. Each region was further probed for the expression of CD11b, 7/4 antigen, MHC-II, CD86, CD62L, CD11c, CD115 and CD209. A similar approach was used on samples obtained from (B) 24, (C) 48h and (D) 72h resolving inflammation as well as (E) inflammation at 72h triggered by 10mg zymosan. Representative figures of four replicates are shown from each time point.

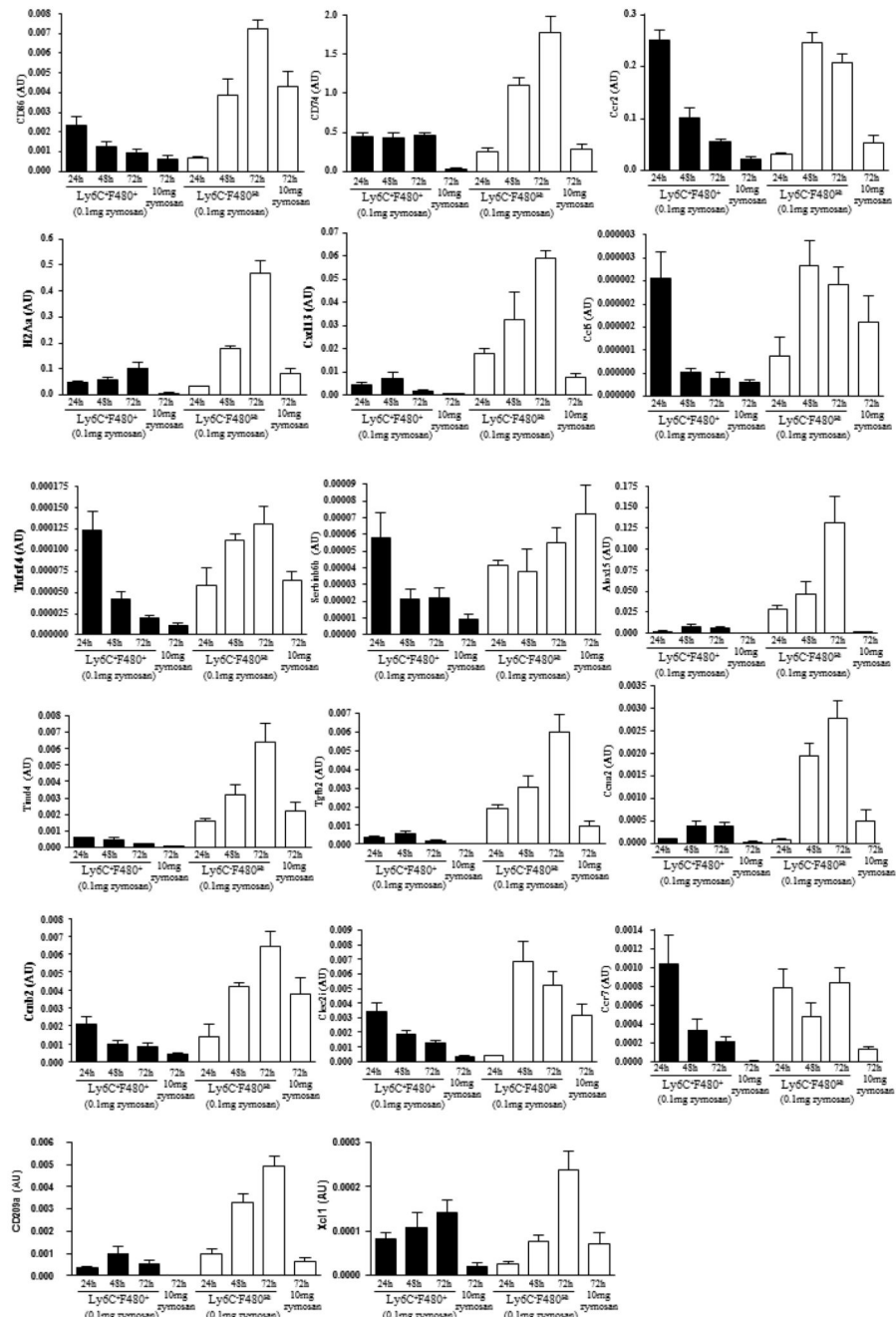
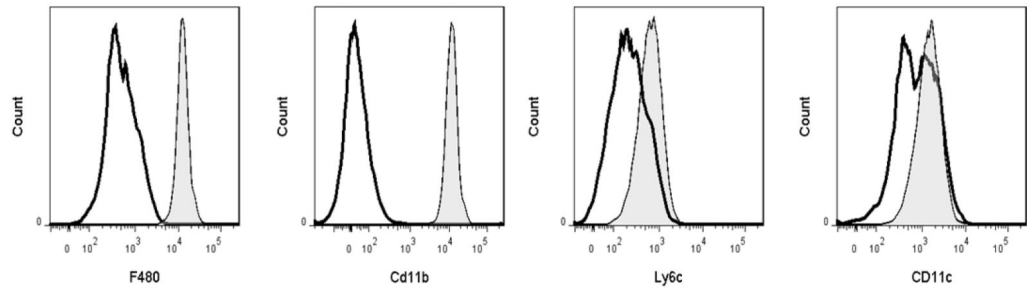


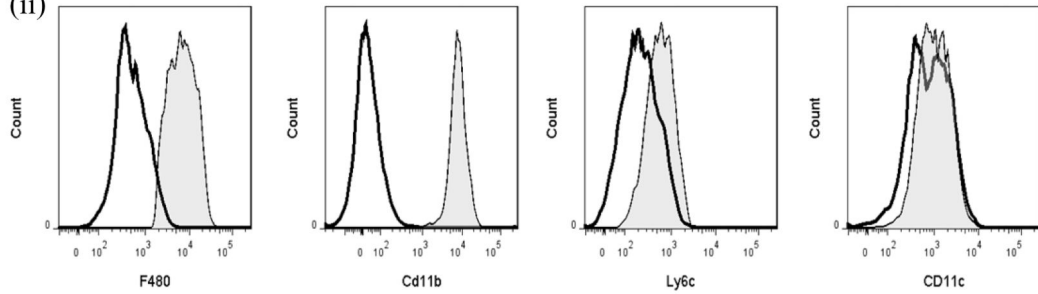
Figure 6. Phenotype of monocytes/macrophage sub-population throughout resolving inflammation.

There are two broad categories of monocytes/macrophages namely Ly6C^{pos}F4/80^{pos} and Ly6C^{neg}F4/80^{hi} revealed in Figure 5B-E. These were isolated using FACSaria at 24, 48 and 72h from resolving peritonitis as well as at 72h from peritonitis triggered by 10mg zymosan. mRNA was extracted and quantitative PCR carried out for the relative expression of genes enriched in each population. Data is expressed as means \pm SEM for n=3-6 replicates per group. Note, cells from these each of these replicates are pooled from 3-5 animals prior to FACS cell sort

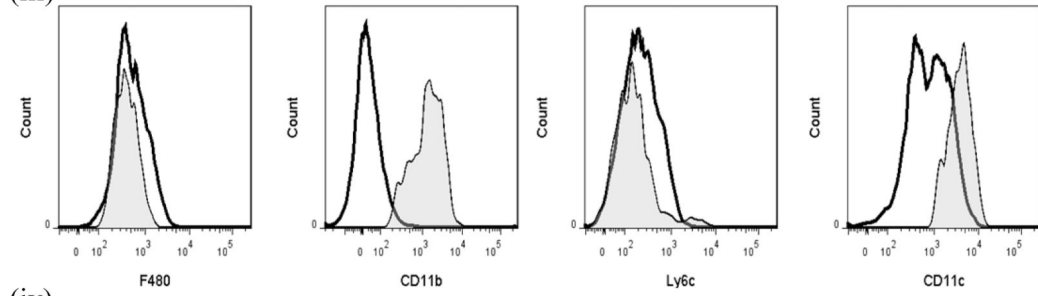
A
(i)



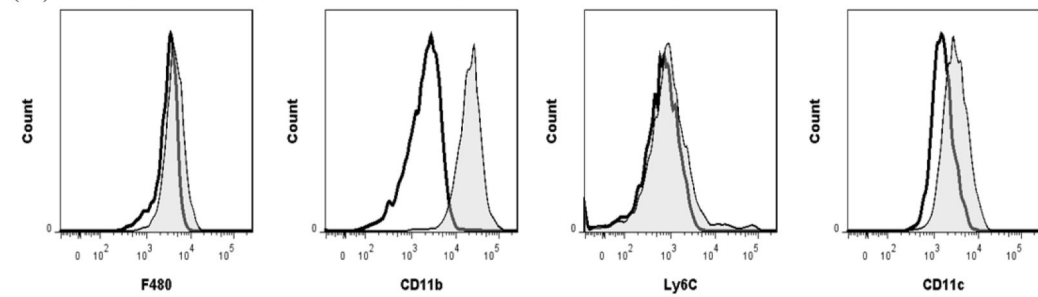
(ii)



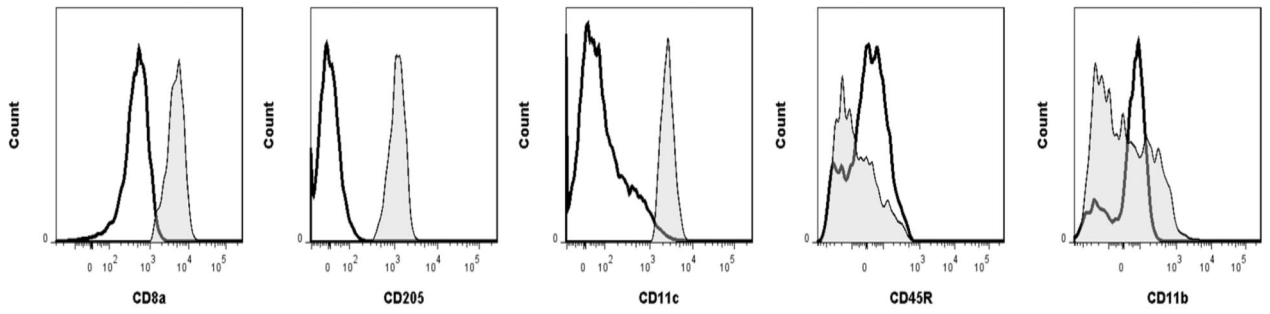
(iii)



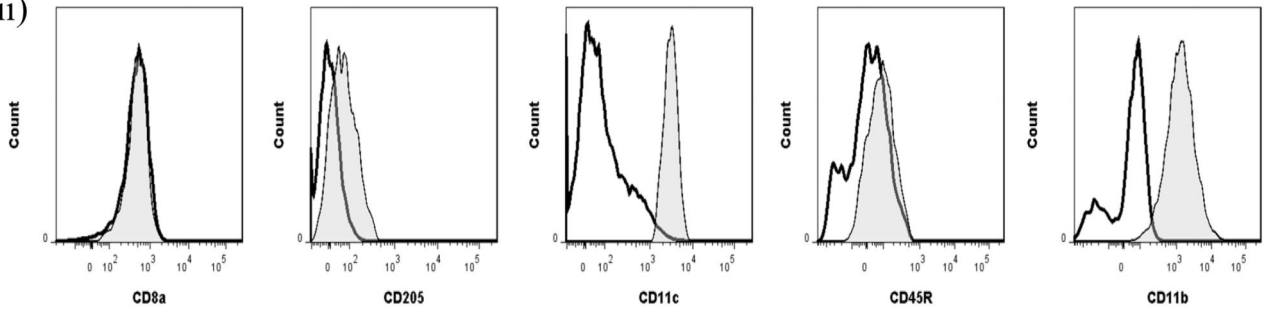
(iv)



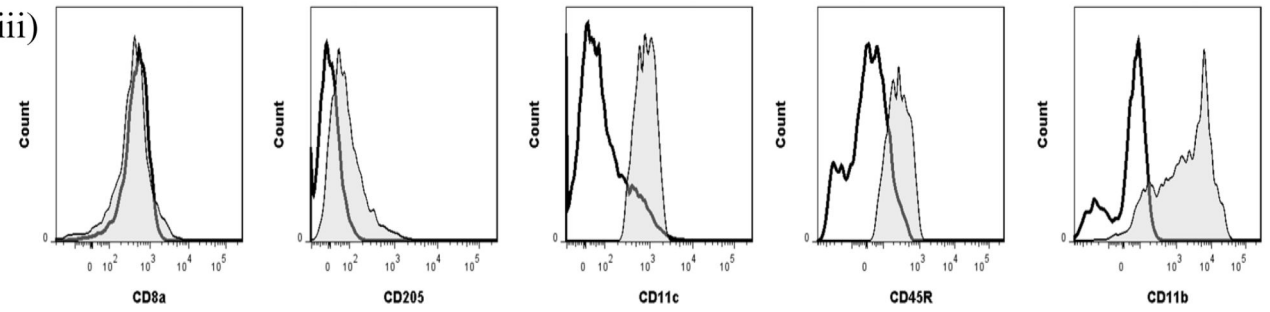
B
(i)



(ii)



(iii)



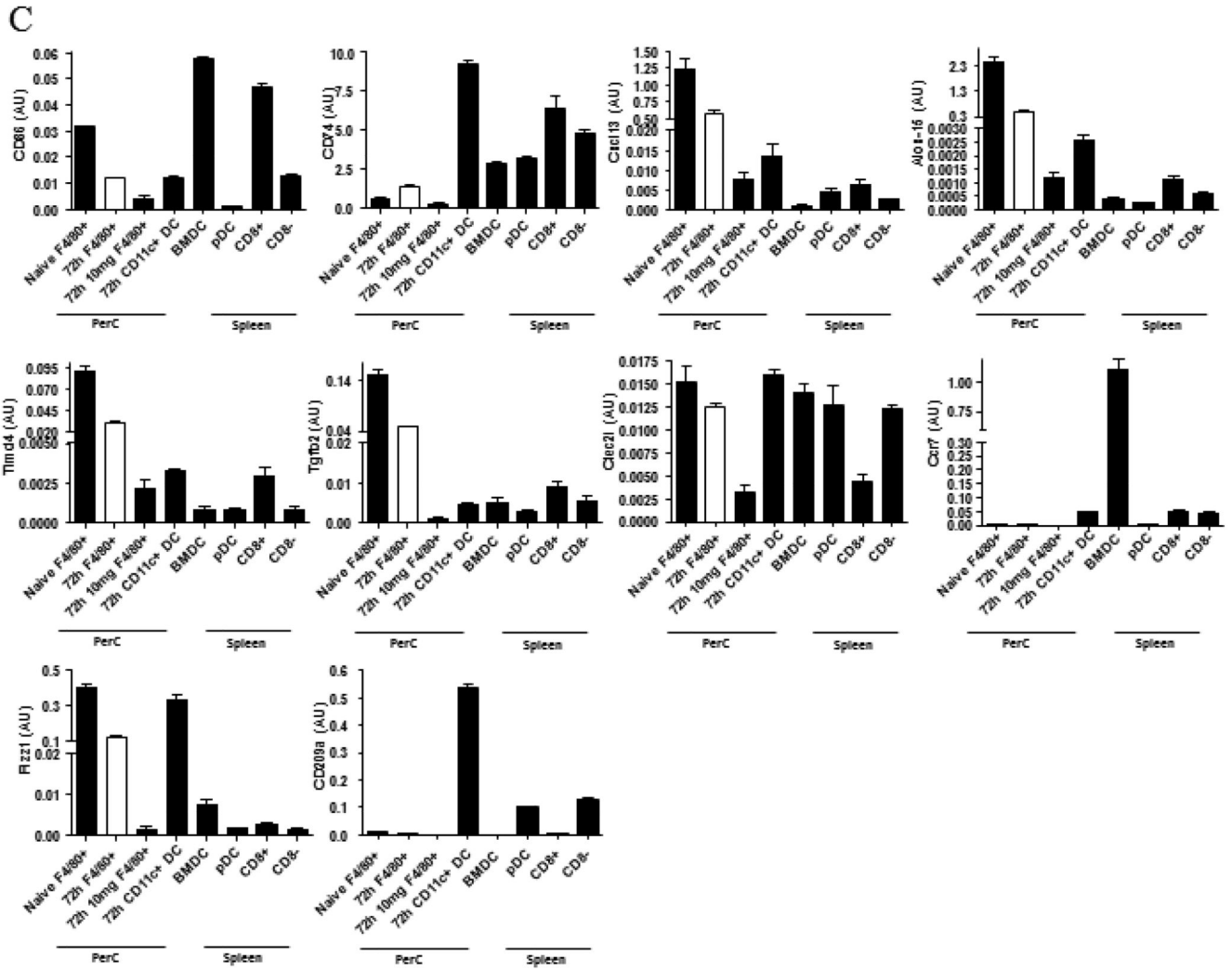


Figure 7. Phenotype of rM compared to conventional dendritic cells.

In panel (A) levels of CD11c expression among other markers was examined on (i) naïve peritoneal macrophages and (ii) rM cells compared to (iii) CD11c-positive cells-FACS-sorted from a 72h resolving peritoneal cavity as well as (iv) GM-CSF/IL-4 generated bone marrow-derived dendritic cells stimulated with LPS. In (B) we characterised (i) CD8^{POS}, (ii) CD8^{NEG} and (iii) plasmacytoid dendritic cells for their (C) comparison of with rM at message level for MHC-II as well as co-stimulatory molecules (CD74 and CD86), monocyte-derived dendritic cells marker (CD209a) and the immune synapse mediator Clec2i among other key rM markers summarised in Figure 3. PerC = peritoneal cavity.

Table 1
Selection of GO terms enriched in the differentially-regulated genes in rM versus naive and pro-inflammatory macrophages identified by VLAD analysis.

For full list of enriched GO terms and the list of the genes in the query set that are annotated to the GO terms see Table S3. In this analysis the regulation GO terms do not have a transitive relationship to the "parent" GO terms, so that there is not a complete overlap between the genes associated with GO:0030335: positive regulation of cell migration and those associated with GO:0016477: cell migration (see Table S3). k = number of genes in the query set annotated to the GO term, or descendants of the GO term. M = number of genes in the background dataset annotated to the GO term, or descendants of the GO term.

GO ID and GO term	FDR0.001 and Fold change>2.0 (37 genes)		FDR0.05 and Fold change>1.5 (342 genes)		
	P-value	k	P-value	k	M
GO:0050896: response to stimulus	1.90E-06	19	5.23E-11	110	5836
GO:0007165: signal transduction	#N/A	#N/A	1.35E-04	64	3905
GO:0010468: regulation of gene expression	#N/A	#N/A	1.28E-10	63	2570
GO:0002376: immune system process	4.19E-07	9	1.19E-16	43	908
GO:0009966: regulation of signal transduction	2.02E-04	7	1.11E-09	37	1142
GO:0042981: regulation of apoptosis	6.31E-05	7	1.58E-09	33	947
GO:0002682: regulation of immune system process	2.04E-07	8	1.26E-12	30	594
GO:0010646: regulation of cell communication	8.45E-04	6	5.03E-06	28	1042
GO:0035556: intracellular signal transduction	#N/A	#N/A	2.50E-06	28	1004
GO:0007049: cell cycle	#N/A	#N/A	8.34E-06	23	780
GO:0030097: hemopoiesis	1.79E-05	5	4.57E-10	19	300
GO:0006952: defense response	1.98E-05	6	2.74E-06	19	522
GO:0031347: regulation of defense response	#N/A	#N/A	5.80E-09	17	276
GO:0007155: cell adhesion	#N/A	#N/A	7.09E-04	16	610
GO:0016477: cell migration	7.10E-04	4	9.65E-06	15	373
GO:0009611: response to wounding	8.63E-04	4	2.63E-04	13	393
GO:0050670: regulation of lymphocyte proliferation	1.12E-05	4	9.35E-09	12	127
GO:0034097: response to cytokine stimulus	3.19E-06	5	2.26E-06	12	210
GO:0030098: lymphocyte differentiation	4.05E-04	3	1.43E-07	11	132
GO:0001817: regulation of cytokine production	#N/A	#N/A	1.05E-04	11	263
GO:0042110: T cell activation	5.22E-04	3	2.81E-06	10	144
GO:0045087: innate immune response	7.10E-04	3	7.21E-06	10	160
GO:0002819: regulation of adaptive immune response	5.31E-08	5	4.25E-08	10	92
GO:0002697: regulation of immune effector process	#N/A	#N/A	9.06E-05	9	174
GO:0030335: positive regulation of cell migration	4.12E-05	4	1.03E-04	9	177
GO:0019882: antigen processing and presentation	3.19E-09	5	7.23E-08	8	53
GO:0045088: regulation of innate immune response	#N/A	#N/A	1.29E-04	8	143
GO:0001666: response to hypoxia	#N/A	#N/A	1.07E-05	8	101
GO:0009615: response to virus	#N/A	#N/A	1.75E-05	8	108

GO ID and GO term	FDR0.001 and Fold change>2.0 (37 genes)		FDR0.05 and Fold change>1.5 (342 genes)		
	P-value	k	P-value	k	M
GO:0042113: B cell activation	#N/A	#N/A	2.60E-04	6	85
GO:0002690: positive regulation of leukocyte chemotaxis	5.27E-04	2	2.86E-04	4	31